A review of the current understanding of seismic shear-wave splitting in the Earth's crust and common fallacies in interpretation

Stuart Crampin [a,b,c,*], Sheila Peacock [d]

[a] *School of GeoSciences, University of Edinburgh, West Mains Road, Edinburgh EH9 3JW, Scotland, UK*
[b] *Edinburgh Anisotropy Project, British Geological Survey, Edinburgh EH9 3LA, Scotland, UK*
[c] *Institute of Earthquake Science, China Earthquake Administration, 100036 Beijing, China*
[d] *AWE Blacknest, Brimpton, Reading RG7 4RS, UK*

Abstract

Azimuthally-aligned shear-wave splitting is widely observed in the Earth's crust. The splitting is diagnostic of some form of seismic anisotropy, although the cause of this anisotropy has been sometimes disputed. The evidence in this review unquestionably indicates cracks, specifically stress-aligned fluid-saturated microcracks, as the predominant cause of the azimuthally-aligned shear-wave splitting in the crust. Although, in principle, shear-wave splitting is simple in concept and easy to interpret in terms of systems of anisotropic symmetry, in practice there are subtle differences from isotropic propagation that make it easy to make errors in interpretation. Unless authors are aware of these differences, misinterpretations are likely which has led to incorrect conclusions and charges of controversy where only misinterpretations exist. As a consequence, stress-aligned fluid-saturated microcracks as the cause of azimuthally-aligned shear-wave splitting in the crust is still not universally accepted despite there being distinguishing features that directly indicate crack-induced anisotropy. This paper reviews observations and interpretations of crack-induced shear-wave splitting and demonstrates that claims for aligned crystals and other sources of shear-wave splitting are due to fallacies in interpretation. This review shows how previous contrary interpretations are resolved and discusses common fallacies and misinterpretations. It is suggested that this new interpretation of shear-wave splitting has such fundamental implications for almost all solid-earth geoscience that it amounts to a *New Geophysics* with applications to particularly exploration and earthquake geoscience but also to almost to all other branches of solid Earth geoscience.
Crown copyright © 2008 Published by Elsevier B.V. All rights reserved.

Keywords: Fallacies in interpretation; New Geophysics; New understanding of fluid/rock deformation; Shear-wave splitting

---

* Corresponding author. Address: School of GeoSciences, University of Edinburgh, West Mains Road, Edinburgh EH9 3JW, Scotland, UK. Tel.: +44 131 650 5110; fax: +44 131 668 3184.
   E-mail addresses: scrampin@ed.ac.uk (S. Crampin), sheila@blacknest.gov.uk (S. Peacock).
   URL: http://www.geos.ed.ac.uk/homes/scrampin/opinion (S. Crampin).

1. Introduction

Shear-waves propagating in anisotropic rocks split into two approximately orthogonal polarisations that travel at different velocities and write characteristic easily-identifiable signatures into three-component seismic wave trains [1]. Such shear-wave splitting (seismic birefringence) *aligned azimuthally* is widely observed in almost all igneous, metamorphic, and sedimentary rocks in the Earth's crust in almost all geological and tectonic regimes [2–6]. There are only a few well-understood exceptions where azimuthally-aligned shear-wave splitting has not been observed in the crust [7]. Such azimuthally-aligned shear-wave splitting was first identified in 1981, in both the crust [8] and the upper-mantle [9]; coincidently and independently, both reported in the same volume of Nature. However, despite 25 years of observations, the causes and interpretation of shear-wave splitting in the Earth's crust are still often misunderstood. This review attempts to resolve some of these misunderstandings.

Note that the phrase 'azimuthally-aligned shear-wave splitting' refers to splitting where the faster split shear-waves are approximately parallel as illustrated schematically in Fig. 1. This distinguishes it from the splitting, observed particularly in exploration seismology in finely-layered sedimentary strata, where the polarisations are controlled by the direction of propagation and are strictly *SV* and *SH*.

Anisotropic symmetries are discussed in Section 2.1, below. The evidence suggests azimuthally-aligned shear-wave splitting observed in the Earth's crust is invariably caused by stress-aligned parallel vertical microcracks. This mechanism has the enormous benefit that the crack geometry has comparatively simple anisotropic symmetry that can be specified by three parameters: (1) orientation of the parallel vertical microcracks, imaged by the strike of the nearly-parallel shear-wave polarisations; (2) crack density imaged, by one hundredth of the percentage of shear-wave velocity anisotropy; and (3) changes in crack aspect-ratios, imaged (less easily) by changes in average time-delays between split shear-waves in a particular range of angles of incidence to the free-surface [7]. Changes in crack aspect-ratios are important as we have shown in a recent more formal review of theory and interpretation in Wave Motion [10] that their behaviour in the Earth's crust demonstrates that the microcracks are so closely-spaced they are critical-systems monitoring the low-level pre-fracturing deformation of *in situ* rock. Consequently, shear-wave splitting is caused by stress-aligned near-vertical microcracks [2–6], and is the key diagnostic of the *New Geophysics*: a new understanding of fluid-rock deformation which has profound implications for many properties of *in situ* rocks [7,10,11]. This review provides the consistent interpretation of shear-wave splitting necessary for understanding and promoting the New Geophysics.
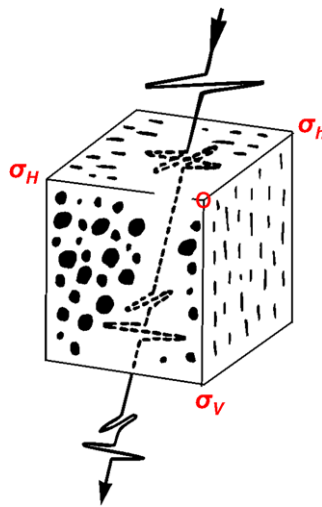

Fig. 1. Schematic illustration of shear-wave splitting through distributions of stress-aligned fluid-saturated parallel vertical microcracks aligned normal to the direction of minimum horizontal stress, σ_h. For propagation within 30° of the vertical, the polarisations of the faster split shear-waves are parallel to the strike of the cracks and parallel to the direction of maximum horizontal stress, σ_H. Such parallel vertical crack orientations are typically found below the critical depth (typically between 500 m and 1000 m), where the increasing vertical stress, σ_V, becomes greater than σ_h, so that the minimum stress is horizontal. (After [6].)

1.1. Background

In 1981, one of us published in Wave Motion [1] a review of theoretical and numerical aspects of wave propagation in cracked and anisotropic media, particularly with reference to observations of anisotropy in the Earth's crust. The most diagnostic feature of azimuthally-aligned anisotropic wave propagation is shear-wave splitting (seismic birefringence), where shear-waves split into differently polarised phases which are azimuthally-aligned, travel at different velocities, and write easily-recognised symbols into polarisation diagrams (PDs), or hodograms, of three-dimensional particle motion. Shear-wave polarisations and time-delays between split shear-waves, the two distinctive parameters in Fig. 1, can easily be identified and measured in PDs.

Azimuthally-aligned shear-wave splitting was positively recognised in *in situ* rock in observations above small earthquakes in Turkey [8,12], and later in seismic reflection surveys, and vertical seismic profiles in oil exploration surveys [13,14] and other reports reviewed by Helbig and Thomsen [15]. Such shear-wave splitting with azimuthally-aligned polarisations is widely observed above small earthquakes (see for example [5,6], and many papers cited throughout this review). Fig. 2 shows an example of shear-wave splitting above a small earthquake in SW Iceland. The horizontal seismograms are rotated into faster and slower shear-wave polarisation directions showing different arrival times. PDs of the horizontal motion of the two split shear-waves show linear motion with a difference in arrival times of ∼0.1 s. The enlarged PD of the horizontal motion shows the linear motion of the faster split shear-wave where the deviations of linearity between the circled shear-wave arrivals are less than the amplitude of the *P*-wave coda. It is interesting that, although shear-wave splitting is a second-order phenomenon of small differences in shear-wave velocities, if split shear-waves are rotated into faster and slower polarisations, as in Fig. 2a, the arrival times can often be read with first-order accuracy.

Azimuthally-aligned shear-wave splitting is also observed in exploration seismology in a huge variety of controlled source experiments in reflection profiles, vertical seismic profiles, and well logs as reviewed in Wave Motion [10].

1.2. The new geophysics

Critical-systems are a New Physics [17]; a New Geophysics. Complex heterogeneous interactive systems initially interact locally, but when they approach singularities, bifurcations, or, in the case of the Earth, fracture-criticality [2], they abruptly display coherent behaviour involving collective organisation of large numbers of degrees of freedom: "It is one of the miracles of nature that huge assemblages of particles subject to the blind forces of nature, are nevertheless capable of organising themselves into patterns of cooperative activity" [18]. Critical-systems and self-organisation are extremely common, including: quantum mechanics; superfluidity; traffic clustering on roads the life cycle of fruit flies; stocks in the New York stock exchange; and a huge number of physical relationships including the Gutenberg–Richter relationship between the logarithm of the cumulative number of earthquakes and the earthquake magnitude, which is linear (self-similar) over at least eight orders of magnitude. Thus, in suggesting that the Earth's crust is a critical-system of stress-aligned fluid-saturated microcracks [11], we are merely suggesting that the Earth behaves like all other complex heterogeneous interactive phenomena.

Critical-systems have a range of behaviour fundamentally different from conventional sub-critical physics (and geophysics), including calculability (hence predictability), extreme ("butterfly wing's") sensitivity to initial conditions leading to deterministic chaos [19]. This implies that fluid-rock deformation in the crack-critical crust of the Earth can be: *monitored* by analysing shear-wave splitting; *modelled* by the anisotropic poro-elasticity (APE) model of fluid-rock deformation (see Section 3); future behaviour *predicted* (if the changing conditions can be quantified); and in appropriate circumstances, future behaviour *controlled* by feedback [11].

These properties are fundamentally different from the sub-critical behaviour of the classic conventional brittle-elastic upper crust. Thus, the understanding of the behaviour of deformation in the Earth's crust has advanced substantially from a conventional brittle-elastic crust to a dynamic compliant self-organised crust. We now know that very small changes in rock mass conditions readily modify the geometry of fluid-saturated microcracks and that these can be monitored by shear-wave splitting. These properties are so different
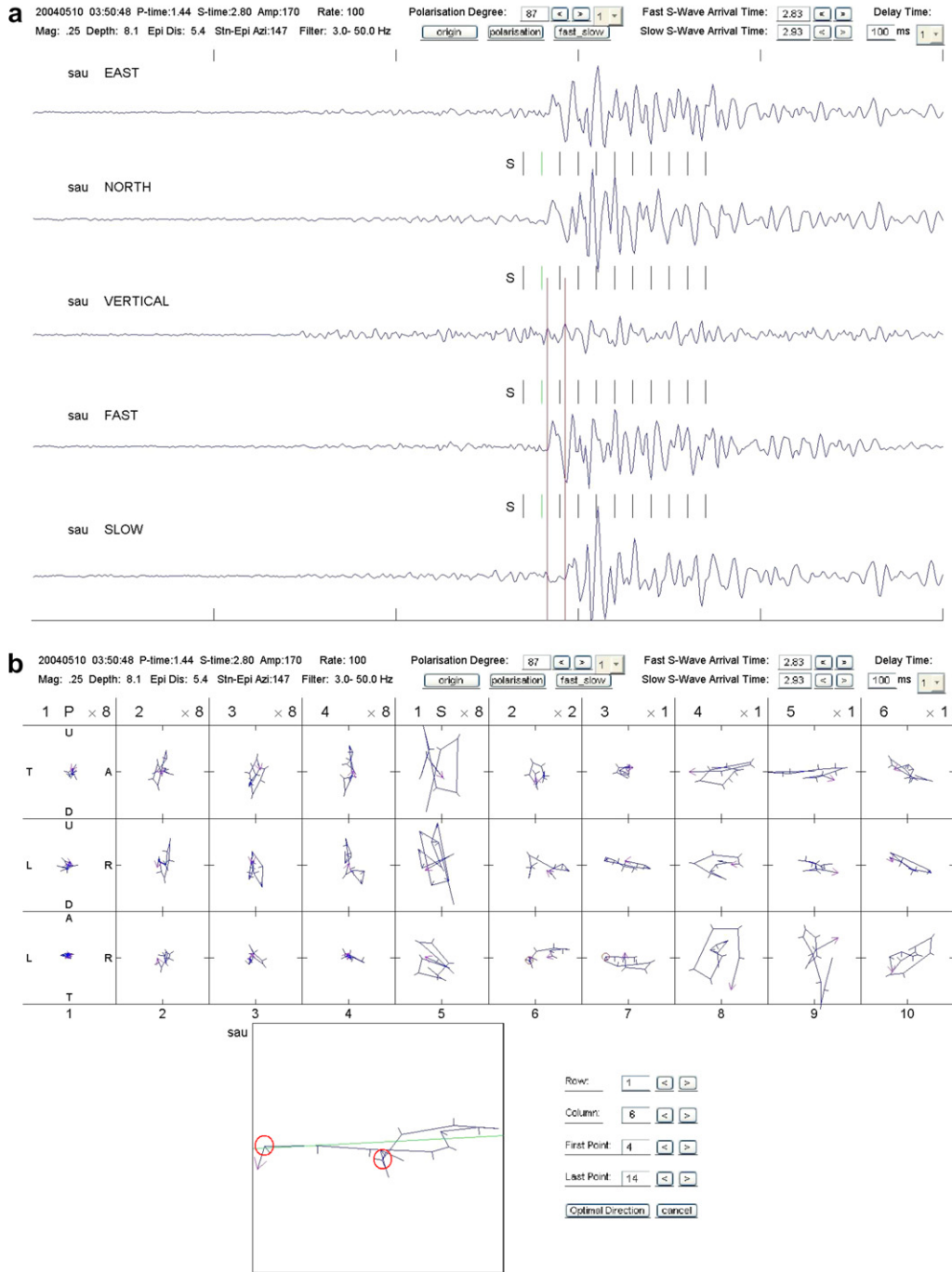
Fig. 2. Shear-wave splitting above a small earthquake (*M* 0.25) at Station SAU in SW Iceland. (a) Seismic traces from top: EW; NS; Vertical; and rotated fast horizontal; and slow horizontal, where azimuths are determined from (b), below. Sampling rate is 0.01 s. Vertical bars following 'S' are numbered 0.1-s intervals for polarisation diagrams (PDs). (b) Mutually-orthogonal PDs, where: U, D, L, R, T, and A refer to Up-, Down-, and Left-, Right-, Towards-, and Away-directions from the source. The number top left is the time interval in (a). Number top right is the relative amplitude factor (number of multiplications of the traces). Sample ticks are to the left of direction of motion. Enlarged horizontal PD shows split shear-waves arrivals where start and end of linear time-delay are circled. (a and b) Screen images from the semi-automatic measuring technique. (After [16].)

from conventional sub-critical behaviour, that many geoscientists are (understandably) reluctant to accept the idea of a highly compliant crack-critical crust of fluid-saturated stress-aligned microcracks, (see for example, a recent book on rock mechanics [20]). A major difficulty for many geoscientists is that the diagnostic effects are almost entirely confined to shear-wave splitting and shear-waves, and the behaviour of shear-wave splitting is only now becoming understood.

1.3. Evidence summarised in this review

This review of azimuthally-aligned shear-wave splitting (seismic birefringence) shows three things:

(1) Azimuthally-aligned stress-aligned shear-wave splitting is almost invariably caused by propagation through distributions of stress-aligned fluid-saturated microcracks, which are highly compliant to small changes of stress.
(2) Stress-induced changes to microcrack geometry can be monitored by variations in shear-wave splitting so that, in particular, at the approach of fracture-criticality, the times and magnitudes of impending larger earthquakes can be estimated by analysing shear-wave splitting.
(3) Characteristic temporal variations of shear-wave time-delays (typically, increases in normalised time-delays, monitoring stress-accumulation, where the logarithm of the duration of the increase is proportional to the magnitude of the impending earthquake) are now seen before earthquakes worldwide (Table 1a).

We refer to such linear log–log relationships as *self-similar*. When there is sufficient seismicity before the impending earthquake to provide shear-wave source events within the shear-wave window (9 cases out of 15 in Table 1b), the increasing time-delays show an abrupt precursory decrease (interpreted as stress relaxation due to cracks coalescing onto the eventual fault break) immediately before the larger earthquake [6]. The durations of these decreases of time-delays are also self-similar with respect to the magnitudes of the impending earthquakes [6,30]. There has been one successful real-time stress-forecast of time, magnitude and fault break of a *M* 5 earthquake in SW Iceland, when the increase in time-delays was recognised before the earthquake had occurred [25]. There are no contrary observations where adequate data sets have not shown characteristic changes before large earthquakes.

We show in the next section (summarised in Table 2) that azimuthally-aligned shear-wave splitting in the crust is almost invariably caused by propagation through stress-aligned fluid-saturated microcracks as illustrated schematically in Fig. 1. Fluid-saturated microcracks are the most compliant elements of the rock mass and crack geometry will readily respond to changes in stress [1,7,41–43]. Consequently, variations in shear-wave splitting are the most sensitive diagnostic indicators of variations in *in situ* microcrack geometry, and such changes have been observed whenever there have been sufficient appropriate shear-wave ray paths before larger earthquakes [5,21–31]. Changes in shear-wave splitting have also been observed before volcanic eruptions [5,32,33,47], and in hydrocarbon reservoirs following fluid-injection [34,35] and possible variations with ocean tides [37].

However, claims that the rock mass is sensitive to small changes of stress is contrary to the concept of the conventional brittle-elastic upper crust and some papers suggest aligned crystal mineralisation as the source of the anisotropy. Some papers suggesting mineral alignments as the cause of shear-wave splitting [48], [49], and [50], have been answered by Crampin [51], [52], and [31], respectively. These various exchanges are summarised in Table 3. Papers [57] and [58] also questioned observations and interpretations of shear-wave splitting, and were answered by Crampin et al. [29]. (Note that [59] suggests that all wholly-automatic measurements of shear-wave splitting are likely to be inadequate.) Paper [60] questioned the statistics of the stress-forecast earthquake [25] and was answered by Crampin et al. [61].

Unfortunately, detailed refutations, however well-founded, seldom receive as much attention as the original criticisms, and misunderstandings and misinterpretations still persist [20,50]. This review discusses a further range of papers reporting shear-wave splitting, and outlines the current understanding. The review demonstrates that the only viable interpretation of azimuthally-aligned shear-wave splitting in the crust is propagation through compliant stress-aligned fluid-saturated microcracks that allow temporal changes in stress to be

Table 1

Reports of temporal variations in shear-wave splitting time-delays in Band-1[a] directions [7]

	Earthquake (EQ) location and date	Magnitude	Approx. duration (days)	Approx. distance (km)	Ref.
	a) Observations of inferred stress-accumulation before earthquakes				
1	Swarm at BRE, N Iceland, 2002	M^b 1.7	$\geqslant 0.055$	7	[6]
2	Swarm at BRE, N Iceland, 2002	M 2.5	$\geqslant 0.21$	7	[6]
3	SW Iceland, 1997	M 3.4	47	10	[5]
4	Dongfang, Hainan, China, 1992	M_L 3.6	21	9	[21]
5	Enola Swarm, Arkansas, USA, 1982	M_L 3.8	4	3	[6,22]
6	SW Iceland, 1997	M 3.8	40	14	[5]
7	Parkfield, California, USA, 1989	M_L 4	$\geqslant 220$	14	[23]
8[c]	SW Iceland, 1997	M 4.4	83, 77	10, 43	[5]
9[c]	SW Iceland, 1998	M 4.7	123, 106	10, 43	[5]
10[c]	Grímsey Lineament, Iceland, 2002	M 4.9	247, 263, 0	50, 92, 96	[20]
11[c]	SW Iceland (successful forecast), 1998	M 5[d]	127, 121	2, 36	[6,25]
12	Shidan, Yunnan, China, 1992	Ms 5.9	400	35	[6,26]
13	N Palm Springs, California, USA, 1988	Ms 6	1100	33	[6,27–29]
14[c]	SW Iceland, 2001	$Ms6.6/M$ 5.6	75, 151	3, 46	[30]
15	Chi–Chi Earthquake, Taiwan, 1999	Mw 7.7	600	55	[31]
	(b) Observations of inferred crack coalescence before earthquakes				
1	Swarm at BRE, N Iceland, 2002	M 1.7	0.0306	7	[6]
2	Swarm at BRE, N Iceland, 2002	M 2.5	0.0465	7	[6]
3	Enola Swarm, Arkansas, USA, 1982	M_L 3.8	0.123	3	[6,22]
4	Grímsey Lineament, Iceland, 2002	M 4.9	24	50	[24]
5	SW Iceland (successful forecast), 1998	M 5	4.4	2	[6,25]
6	Shidan, Yunnan, China, 1992	Ms 5.3	38	35	[6,26]
7	N Palm Springs, California, USA, 1988	Ms 6	69	33	[6]
8[c]	SW Iceland, 2001	M 5.6/$Ms6.6$	38, 21	3, 46	[30]
9	Chi–Chi Earthquake, Taiwan, 1999	Mw 7.7	131	55	[31]
	c) Observations of inferred stress-accumulation before volcanic eruptions				
1[c]	Gjàlp,Vatnajökull Ice Field, Iceland, (increasing time-delays), 1996	Large fissure eruption	120, 120, 120	230 S, 240 SW, 245 WSW	[5]
2[c]	Mount Etna, Sicily (increasing and decreasing time-delays and 90°-flips), 2001	Minor eruption	66[e]	1, 5	[32]
3[c]	Mount Ruapehu, New Zealand (90°-flips), 1992–2002	Minor eruption	–	2–15	[33]

	Location	Observations and interpretation	
	d) Observations of changes in time-delays elsewhere		
1	Vacuum Field, New Mexico, USA	Changes in split shear-waves in reflection surveys after high-pressure and low-pressure CO_2-injections in a hydrocarbon reservoir. High-pressure injections cause 90°-flips in shear-wave polarisation. Shear-wave splitting exactly modelled by APE at correct injected pressures.	[34,35]
2	Observations at 4–9-km depth in the KTB well, SE Germany	Fluid-injection at 9-km depth induced microseismicity which showed a $\sim 2\%$ decrease in time-delays to recorders at 4-km depth.	[36]
3	Borehole observations of induced events in N. Sea oil field	Analysis of borehole records of shear-wave splitting from acoustic events during hydrocarbon production show evidence of changes with ocean tides.	[37]
4	SMSITES experiment: cross-borehole transmission parallel to Húsavík-Flatey (Mid-Atlantic Ridge) transform fault in N Iceland	Travel times of P-, SH-, SV-, SV-SH-waves at 500-m depth between boreholes offset 315 m, NS and EW GPS, and water-well level changes all show great sensitivity to low-level seismicity (106 events $M \leqslant 2.8$ approximately equivalent to one $M3.5$, say) at 70 km distance.	[38]

Table 1 (*continued*)

	Location	Observations and interpretation	
5	Surface observations of small events induced by hydraulic pumping in a hot-dry-rock experiment, Cornwall, UK	Initial pumping tests showed shear-wave polarisations parallel to measured stress directions, whereas polarisations after hydraulic fracturing began were 7° different and parallel to joints and fractures in granite outcrops.	[39]
6	Variation of time-delays with fluid-injection near Krafla Volcano, Iceland, and at Cocos Geothermal Field, CA, USA.	Initially large values of time-delays (normalised to path length) are found to decrease during fluid-injection both at Krafla Volcano, Iceland, and Cocos Geothermal Field, California. This behaviour is not yet understood, but attributed to effects of high pore-fluid pressures.	[40]

[a] Band-1 directions are ray paths in the double-leafed solid angle between 15° and 45° to the plane of the average crack.
[b] Iceland Seismic Network *Bulletins* magnitude where $M \approx mb$.
[c] Observed at a network of stations.
[d] Older magnitude value compatible with other listed magnitudes, given as M 4.9 in current catalogue.
[e] As interpreted by this paper.

monitored by changes in shear-wave splitting. This review also establishes that, whenever there are adequate source data, characteristic patterns of behaviour of shear-wave time-delays are observed before larger earthquakes. Again there are no contrary observations.

2. Azimuthally-aligned shear-wave splitting

The polarisations of split shear-waves in a homogeneous anisotropic medium vary in three dimensions but are fixed for propagation along any particular ray path direction. The time-delays depend on the length and the degree of velocity anisotropy along the ray path. For shear-waves observed within the shear-wave window at the free-surface there are three distinct discriminatory patterns of anisotropic shear-wave polarisations. The first is in hexagonal symmetry (transverse isotropy) with a *vertical* axis of cylindrical symmetry where split shear-wave are always strictly *SV*- and *SH*-wave polarisations, and hence are always parallel or perpendicular to the direction of propagation. The second pattern (the subject of this review) is in hexagonal symmetry with a *horizontal* axis of symmetry where split shear-wave polarisations are parallel in a broad band of directions across the centre of the shear-wave window. We refer to this as azimuthally-aligned shear-wave splitting. The seldom observed third pattern is where polarisations vary with azimuth and incidence angle of the ray path to the surface. These variations are found in all other symmetry systems and in all other orientations of hexagonal symmetry. In this pattern, polarisations usually vary rapidly with angles of incidence and azimuth, and cannot be mistaken for the first two patterns, unless the anisotropic symmetry systems are very similar.

2.1. Origins of azimuthally-aligned shear-wave splitting

Note the caveat *azimuthally-aligned*. Horizontally-stratified structures display shear-wave splitting into purely *SV*- and *SH*-polarisations with no azimuthal variations. Such media include propagation in finely-layered sedimentary sequences in hydrocarbon exploration surveys [62–64]; shales, clays, mudstones, where pore-space is typically constrained between horizontal platelets frequently of mica aligned during deposition [65,66]; and horizontal layering in crust and the upper-mantle [67]. When the wavelength of the shear-wave is greater than the dimensions of the inclusions or the separation of the layers, the anisotropic symmetry of these configurations leads to transverse isotropy (hexagonal anisotropic symmetry) with a *vertical* axis of symmetry, sometimes referred to as TIV- or VTI-anisotropy. In such TIV media, shear-waves split into strictly *SH*- and *SV*-polarisations, where the *SV*-polarisation radiates with the ray path from the source with no velocity variation in the horizontal plane and with no anisotropy-induced azimuthal variations. Since hydrocarbon reservoirs are often in finely-layered sedimentary basins, TIV-anisotropy is frequently observed in seismic exploration.

Table 2
Summary of the main reasons why *stress-aligned* shear-wave splitting is highly indicative of distributions of stress-aligned fluid-saturated microcracks

	Observed phenomena	Interpretation	Ref.
[R1]	Worldwide observations of azimuthally-aligned shear-wave splitting at the surface above small earthquakes in all types of rock and terrain typically show polarisations of the faster split shear-wave aligned approximately parallel (or occasionally orthogonal – see [R5], below) to the direction of the maximum horizontal stress, σ_H.	The only anisotropic symmetry system with leading to parallel polarisations within the shear-wave window at the surface is hexagonal symmetry with a horizontal axis of cylindrical symmetry, or a minor variation thereof. The only common geological phenomenon having such symmetry is fluid-saturated stress-aligned microcracks which (like hydraulic fractures) tend to be aligned perpendicular to the direction of minimum compressional stress [77]. Polarisations above earthquakes are only approximately aligned because of disturbances to microcrack geometry caused by high pore-fluid pressures on all seismogenic faults (see [R5], below).	[1,5,7,10,41,42]
[R2]	Temporal variations in shear-wave time-delays have been observed (in retrospect) before some 15 earthquakes with magnitudes M 1.7 to M 7.7 (including one real-time successful stress-forecast of time, magnitude, and location) (Table 1). Whenever there is adequate data, these characteristic patterns of temporal variation are seen before all larger earthquakes.	Fluid-saturated microcracks are the most compliant elements of the rock mass. All other sources of anisotropy are likely to be fixed or vary more slowly. Only fluid-saturated microcracks can rapidly respond to changes of low-level stress. (Note that these patterns of behaviour are typically in very sparse data sets and can rarely be quantified statistically.)	[5–7,21,41–43]
[R3]	The Anisotropic Poro-Elastic (APE) model of evolution of fluid-saturated microcracks approximately matches 15–20 different observational phenomena (and innumerable individual source-to-geophone ray paths) above small earthquakes and in seismic exploration operations pertaining to cracks, stress, and shear-wave splitting.	The underlying rationale of APE assumes a critical-system of fluid-saturated grain-boundary cracks and aligned pores and pore-throats in all sedimentary, igneous, and metamorphic rocks in the crust. Hence, the approximate match of APE to observations is strongly indicative of distributions of critical-systems of fluid-saturated microcracks in almost all crustal rocks. The matches are only approximate because of the difficulty of getting accurate *in situ* measurements of crack parameters at depth in the crust.	[11,41–43]
[R4]	Temporal variations in shear-wave splitting have been observed in both high- and low-pressure CO_2-injection in a fractured carbonate hydrocarbon reservoir. The variations are matched exactly by synthetic seismograms modelled with APE for appropriate injection pressures.	This direct match of fluid-rock interaction strongly indicates critical-systems of compliant stress-aligned fluid-saturated microcracks. These results are the best *in situ* calibration of the APE model to-date.	[34,35]
[R5]	Earthquakes appear to occur when temporal variations in time-delays reach levels of fracture-criticality.	A necessary condition for fracturing is that cracks are so closely-spaced (at fracture-criticality) that shear-strength is lost and rocks fractures whenever there is any disturbance.	[2,5–7]
[R6]	Evidence for 90°-flips in shear-wave polarisations is observed above all seismogenic faults and in critically-high-pressurised reservoirs.	These highly distinctive diagnostic changes can be modelled by APE as the effects of stress-induced modifications to compliant critical-systems caused by critically-high pore-fluid pressures on all seismogenic faults.	[5,35,44,45]
[R7]	Observations of time-delays above small earthquakes typically show a ±80% scatter about the mean, which does not occur for controlled source observations away from seismogenic faults.	These well-established observations cannot be explained by conventional (sub-critical) geophysics but (assuming critical-systems of cracks) can be modelled by APE as 90°-flips in shear-wave polarisations caused by critically-high pore-fluid pressures rearranging local microcrack orientations surrounding all seismogenic faults.	[5,44,45]

References to items in this table will be referred to as [R?].

Table 3
Summary of earlier contrary interpretations denying compliant fluid-saturated microcracks; previous comments, and originator's responses

Contrary interpretations	Summary of previous comments	Summary of originator's response
1) Brocher and Christensen [48] interpreted 20% *P*-wave velocity anisotropy in an azimuthally-varying reflection–refraction survey in the highly irregular topography of the Chugach Terrane in Southern Alaska as caused by heavily-foliated schists.	Crampin [51] suggested that *P*-wave arrival times are sensitive to so many different phenomena that wandering multidirectional surveys in extreme topography are difficult to interpret reliably. Several possible misinterpretations in [48] are suggested by Crampin [51]. In particular, foliated schists causing *P*-wave velocity anisotropy require nearly uniform alignments over a large complicated area. This is highly unlikely and unproven. Aligned cracks are the default interpretation.	Brocher and Christensen [51] repeated their original arguments for heavily-foliated schists. *This review's comments: Table 2 [R1, R2] suggests that crack anisotropy must be the default interpretation for azimuthally-aligned anisotropy in the crust unless there is direct evidence otherwise. Neither the original Paper [48] nor their response to our comments (included in) [51] presented other evidence.*
2) do Nascimento et al. [49] observed shear-wave polarisations, above very shallow earthquakes in Brazil, which were orthogonal to the direction of maximum tectonic stress and hence, they suggest, cannot be caused by stress-aligned fluid-saturated microcracks, which are parallel to stress.	Crampin [52] notes that all the earthquakes of [49] are exceptionally shallow (2–5-km deep). Most studies of shear-wave splitting use source earthquakes below 5-km depth. Thus the orthogonal polarisations in [49] are likely to be 90°-flips, caused by the critically-high-pressures found on all seismogenic faults, where the normally pressurised paths above the faults are too short to remove flipped polarisations around the fault [44,45].	The response of do Nascimento et al. [53] does not counter arguments of [52], but

In contrast, whenever there are appropriate source-to-receiver geometries, near-parallel azimuthally-aligned shear-wave splitting, the second pattern, is always observed throughout the Earth's crust with the faster split shear-waves polarised typically in the direction of maximum horizontal stress. There are two inescapable implications. Firstly, the *only* anisotropic symmetry system that produces such parallel polarisations (within the shear-wave window at the surface) is *transverse isotropy of (hexagonal anisotropic symmetry) with a horizontal axis of symmetry*, or a minor variation thereof [1,7,68]. This is often referred to as TIH- or HTI-anisotropy. Secondly, the *only* geological configuration common to sedimentary, igneous, and metamorphic rocks that has TIH-anisotropy, is *stress-aligned fluid-saturated microcracks* [15,69], at one time referred to as *extensive-dilatancy anisotropy* or *EDA-cracks* [70]. These two implications are paramount. Azimuthally-aligned shear-wave splitting, where the leading polarisation is parallel (or occasionally orthogonal) to the stress-field, is almost invariably caused by parallel vertical stress-aligned microcracks. No other mechanisms are possible except in exceptional conditions. Consequently, the default interpretation of azimuthally-aligned shear-wave splitting with parallel polarisations is necessarily in terms of systems of stress-aligned fluid-saturated microcracks.

Such fluid-saturated microcracks are the most compliant elements of *in situ* rocks. In principle, microcracks in strongly aligned minerals might modify microcrack orientations, but this has not been demonstrated in practice. With minor exceptions, we know of no adequate demonstrations of other sources of shear-wave splitting for wholly crustal ray paths, except for well-understood observations of the first polarisation pattern of TIV-anisotropy in exploration seismology. Henceforth, all references to shear-wave splitting in this paper will refer to azimuthally-aligned crack-aligned shear-wave splitting with TIH-anisotropy.

Anisotropy caused by fluid-saturated microcracks is confirmed by observations of *temporal* variations in

complicated and heterogeneous. Even at the specimen scale, Babuška [75] notes that rock samples that are seismically isotropic often have mineral alignment obvious to the eye. He attributed this to the anisotropies of different mineral species cancelling each other when they are all aligned by the same stress-field.

More technically, the comparatively-narrow upper and lower limits of shear-wave velocity anisotropy uniformly observed in all types of rock (1.5% and 4.5% [2,5,7]) are difficult to reconcile with crystal anisotropy as the main cause of the observed shear-wave splitting. The theoretical limits of crystal anisotropy are from zero (randomly aligned with no anisotropy) to the frequently very large single crystal anisotropy of a mineral (over 100% for some micas [76]). Consequently, aligned crystalline minerals are unlikely to be the cause of the comparatively-uniform low values of shear-wave splitting almost universally observed in the crust. Of course, it is possible that a chance combination of circumstances might lead to mixtures of crystals with the same parallel alignments of shear-wave polarisations and the same percentages of velocity anisotropy. However, this is untenable for the huge variety of *in situ* rocks where azimuthally-varying shear-wave splitting has been observed, and no such source has been identified (see Appendices A, B, C, D, E, below). Consequently, the default explanation for the cause of the widely observed parallel shear-wave polarisations is necessarily stress-aligned fluid-saturated *microcracks*. Seven reasons why parallel stress-aligned shear-wave splitting indicates fluid-saturated stress-aligned microcracks are summarised in Table 2.

Fluid-saturated cracks (and hydraulic fractures) tend to open and remain open perpendicular to the direction of minimum compressional stress [77]. At the surface, the minimum stress is typically vertical so that near-surface cracks (and fractures opened by hydraulic pumping) may be horizontal. As the vertical stress increases with overburden, a critical depth is reached, usually between 500 m and 1500 m, where the vertical stress, σ_V, equals the minimum horizontal stress, σ_h. Below this depth, the minimum stress is typically horizontal and microcracks (and hydraulic fractures) are aligned parallel and vertical, normal to the direction of minimum horizontal stress and strike approximately parallel to the direction of maximum horizontal stress, σ_H, yielding TIH-anisotropy as shown schematically in Fig. 1 [77]. Although the general behaviour of both body- and surface-wave propagation in anisotropic rocks has been understood for many years [1,78], the cause of the shear-wave splitting in almost all rocks in the crust (fluid-saturated stress-aligned cracks and microcracks) is still questioned. This is perhaps surprising in view of the irrefutable arguments in this section and Table 2. This present review of the preferred understanding of azimuthally-aligned shear-wave splitting demonstrates that the azimuthally-aligned shear-wave splitting along crustal ray paths is almost invariably caused by stress-aligned cracks and microcracks.

2.2. Five additional phenomena associated with shear-wave splitting and seismic anisotropy

1) There are a large number of papers reporting observations of azimuthally-aligned shear-wave splitting in seismic exploration literature. These observations and applications are exclusively interpreted as caused by fluid-saturated stress-aligned cracks [15]. It is only in the context of earthquake seismology and upper-mantle anisotropy that other interpretations have been suggested which we review in the Appendices.

2) The *shear-wave window* at a horizontal free-surface is the solid angle of incidence directions with radius $\sin^{-1} Vs/Vp (=\sim 35°$, for a Poisson's ratio of 0.25) within which the apparent velocity of shear-waves, parallel to the surface, is so great that *S*-to-*P* conversions cannot occur for incident *SV*-waves on a (horizontal) free-surface [79–81]. Outside the window, the waveforms of shear-wave arrivals are so seriously disturbed that meaningful *SV*-wave arrival times are unreadable, although SH-wave arrivals are not altered. Consequently, shear-wave splitting on surface-recorded seismograms in the field, must be necessarily observed within the shear-wave window at the free-surface at incidence ray path angles of less than about 35°. However, weathering and stress release anomalies tend to lower near-surface velocities and make seismic rays curve upwards. Such velocity reductions often lead to an effective shear-wave window typically out to (straight-line) incidence of 45° or 50°. In practice, the effects of the shear-wave win-

3) *P*-waves, unlike shear-waves, do not have distinctive diagnostic behaviour indicating propagation through anisotropic solids. Anisotropy does cause *P*-wave velocity anisotropy, but *P*-wave travel times are sensitive to so many phenomena that purely anisotropy-induced effects are difficult to isolate. *P*-waves are usually only marginally affected by thin fluid-saturated microcracks [83] and small changes in microcrack geometry are generally invisible to *P*-wave propagation through thin cracks. Consequently, variations in shear-wave splitting are key observables for recognising and quantifying stress-aligned anisotropy in the crust.

4) The human eye has little ability to interpret polarisation information in multi-component "wiggly-line" seismograms. However, shear-wave splitting writes characteristic signatures into polarisation diagrams (PDs, or hodograms) of abrupt nearly-orthogonal changes in particle motion direction, and the human eye does have the ability to recognise patterns in two-dimensional PDs (as in Fig. 2) in many difference circumstances. Experience of interpreting both field and synthetic seismograms suggests that visual inspection of PDs is an optimal way to identify and measure shear-wave splitting arrivals.

5) However, plotting and measuring PDs is time-consuming and tedious. Consequently, many authors have devised various automatic or semi-automatic techniques for measuring the parameters of shear-wave splitting. In a review of such techniques, [59] suggests that wholly-automatic techniques are never likely to be wholly successful except on high signal-to-noise ratio near-classic examples of shear-wave splitting, which in most circumstances are infrequent. This means that data has to pass rigorous selection criteria that sometimes exclude 50% to 70% of the original arrivals before fully automatic techniques can be used to reliably measure shear-wave splitting [84]. Such severe selection can seriously bias any interpretation and such wholly automatic techniques are best avoided.

Consequently, Gao et al. [12] have developed a Shear-Wave Analysis System (SWAS) for *semi-automatic* measurement of shear-wave splitting. Using an Expert Analysis System for initial picks of shear-wave arrivals, the picks are optimised by switching between screen images of: PDs; original NS and EW horizontal seismograms; and seismograms rotated into preferred orientations, in a user-friendly environment, thus combining the advantages of previous techniques (Fig. 2 shows screen images of this process). SWAS reduces the time taken for visual measurements by a factor between 10 and 50, and obtains satisfactory measurements for ~85% of arrivals [16]. Developed for interpreting seismograms from the SIL seismic network in Iceland [85,86] via Internet data, it is intended that SWAS will be generally available for measuring and analysing shear-wave splitting.

3. A brief review of the properties of fluid-saturated microcracks in the earth's crust

The crack density of a uniform distribution of parallel microcracks is $\varepsilon = N\,a^3/V$, where N is the number of cracks of radius a in volume V [2,46,88–90]. This crack density is approximately equal to one hundredth of the percentage of shear-wave velocity anisotropy in aligned cracks in a medium with a Poisson's ratio of 0.25 [2,87]. Thus, the observed percentage of shear-wave velocity anisotropy in intact unfractured rock, the narrow range 1.5–4.5%, can be equated to the narrow range of crack density $\varepsilon = 0.015$–0.045 [2,7,88].

Fig. 3 is a schematic (dimensionless) illustration of observed distributions of fluid-saturated microcracks in ostensibly intact rock [2] that have the observed shear-wave velocity anisotropy of 1.5–4.5%. Fig. 3 suggests that between crack densities of $\varepsilon = 0.045$ and 0.1 there is a level of fracture-criticality when cracks are so closely-spaced that shear-strength is lost and rocks fracture if there is any disturbance. Fracture-criticality is now approximately identified with fluid-percolation threshold when cracks are so closely-spaced there are through-going fractures [2,10,42,43]. At fracture-criticality, fracturing and earthquakes necessarily occur whenever the rock mass is disturbed in any way.

3.1. Modelling fluid-rock evolution with anisotropic poro-elasticity (APE)

The evolution of such highly compliant fluid-saturated microcracks in response to changing conditions can be modelled by *anisotropic poro-elasticity* (*APE*) [41,42], where the mechanism for deformation is fluid movement by flow or dispersion along pressure gradients between neighbouring microcracks at different
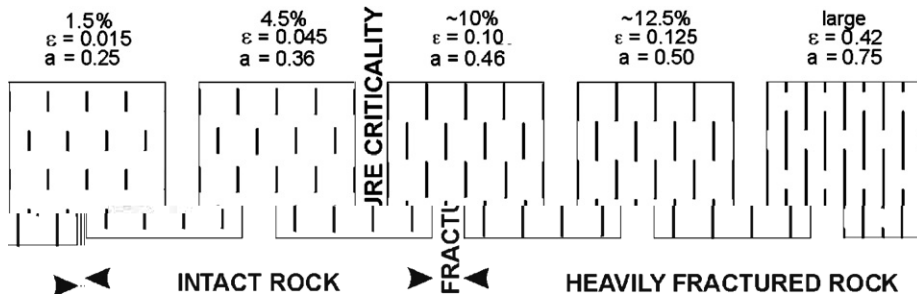
Fig. 3. Cross-sections of uniform dimensionless distributions of parallel stress-aligned fluid-saturated microcracks representing observed shear-wave velocity anisotropies in percent (~1.5% to ~4.5%), crack density ε, and crack radius a, where ε is equal to one hundredth of percent shear-wave velocity anisotropy. Fracture-criticality is at $\varepsilon = \sim 0.055$ (~5.5% shear-wave velocity anisotropy) [38]. (After [2].)

orientations to the stress-field. Fig. 4 gives a schematic (dimensionless) illustration of APE-modelling increasing stress in distributions of vertical randomly aligned fluid-saturated microcracks. Hexagons are elastically isotropic so that the two solid hexagons in Fig. 4 are a small selection of randomly oriented cracks.

APE-modelling helps to explain the lower and upper bounds of shear-wave velocity anisotropy: as increasing stress begins to align fluid-saturated intergranular cracks for initially very low-levels of stress, although some fluid moves round each grain there is initially no crack closure and no effective anisotropy. However, when a critical stress, normalised to one in Fig. 4, bottom left, is reached and cracks first begin to close, the anisotropy immediately jumps from isotropy (no splitting) to approximately the 1.5% minimum shear-wave velocity anisotropy actually observed. The lower left image in Fig. 4 is similar to the left-hand image
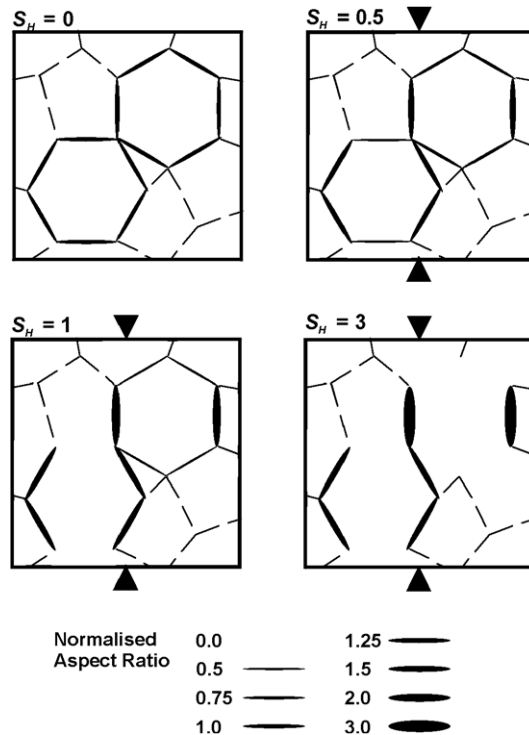

Fig. 4. Schematic illustration of APE-modelling the evolution of crack aspect-ratios in an initially random distribution of vertical cracks (solid lines) for four values of increasing maximum horizontal differential stress, σ_H, normalised to the critical value at which cracks first begin to close. Minimum horizontal stress, σ_h, is zero. Pore-fluid mass is preserved and aspect-ratios are chosen to give a porosity of $\phi \approx 5\%$. Paper [39] gives a detailed interpretation. (After [39].)

in Fig. 3, showing that the two approaches are compatible. The upper bound in intact unfractured rock, ~4.5%, is close to the fluid-percolation threshold, which for parallel cracks is approximately 5.5%, $\varepsilon = 0.055$ [42].

Note that conventional dilatancy, stress-induced opening of new cracks, is a high stress phenomenon. Whereas APE-modelling is an extremely low-stress phenomenon: the critical stress in Fig. 4 must be low as stress-aligned shear-wave splitting is observed in almost all *in situ* rocks, regardless of the level of tectonic stress.

APE-modelling in Fig. 4 is highly constrained yet approximately matches a large (20+) range of different phenomena [7,10,11,42–45]. The reason for this universality is that microcracks in the Earth's crust are so closely-spaced they verge on fracture-criticality and fracturing, as indicated in Fig. 3. Verging on critical points (singularities or bifurcations) is one of the defining characteristics of critical-systems. Critical-systems are a New Physics, *a New Geophysics*, where the statistics are nearer to those of other critical-systems than they are to the specific sub-critical physics and much of the behaviour is calculable [7,10,11,18,19,41,42,91,92]. The universality of critical-systems is the underlying reason that APE-modelling, with minimal parameters, matches such a wide range of phenomena. This behaviour has been reviewed by Crampin and Peacock [10].

The clearest quantifiable demonstration of stress-induced changes in shear-wave splitting in exploration seismology is during hydraulic pumping in a hydrocarbon reservoir [34], where the response was accurately modelled by APE [35].

3.2. Variation of time-delays with direction: band-1 and band-2

The most sensitive response of fluid-saturated stress-aligned microcrack geometry to low-level increases of stress during stress-accumulation before earthquakes is increasing crack aspect-ratios [7,42,43]. Such changes in aspect-ratio can be monitored by changes in the *average* time-delay in Band-1 directions within the shear-wave window [7]. Band-1 is the double-leafed solid angle of ray path directions making angles 15° to 45° to the average crack plane. For thin cracks, Band-1 has a range of positive time-delays, but also includes a small solid angle of negative time-delays, so that averages need to be taken to estimate increases or decreases when the actual ray paths cannot be exactly identified. Band-2 is the solid angle of ray path directions ±15° to either side of the average crack plane which is sensitive to crack density but is insensitive to changes in aspect-ratio. Fig. 5 shows the ray path geometry for Band-1 and Band-2 directions. Only changes in crack density will significantly change time-delays in Band-2 [7], and crack density is insensitive to low-level deformation [42,43].

Fig. 6 shows temporal increases and precursory decreases in normalised time-delays before six earthquakes ranging in magnitude from a *M* 1.7 swarm event in Northern Iceland [6], to the *Ms* 6 1986 North Palm Springs Earthquake in California [27–29]. The consistency of the left-hand and right-hand images is strong confirmation that shear-wave splitting is modelling earthquake source related phenomena.

3.3. Negative time-delays

The shear-wave time-delay is the difference in arrival time between the two split shear-waves. Positive time-delays are usually taken as those when the polarisation of the faster split shear-waves are parallel to the planes of the parallel cracks. When the faster and slower arrivals exchange polarisations, as in 90°-flips [35,37,44], the sign of the time-delays reverses. There are several common situations when this occurs.

(1) When the velocity variations of the two waves intersect at the point-singularities common to all systems of anisotropic symmetry (except hexagonal symmetry, which has line-singularities) [93]. This behaviour showing exchanges of polarisations has been theoretically modelled [94,95] and has been observed and modelled in multi-offset VSPs in the Paris Basin [96].
(2) When the directions of shear-wave ray paths cross line-singularities in systems of hexagonal symmetry, such as that of parallel microcracks [94]; see observations in Sections B2.5, D2.2 and D2.3.
(3) When microcrack orientations are re-arranged in the presence of critically-high pore-fluid pressures in hydrocarbon reservoirs causing 90°-flips in shear-wave polarisations [35,95] and on seismically-active fault lines [38,44,45].
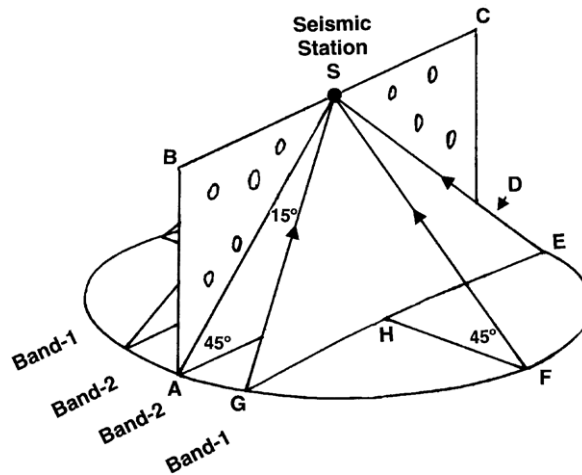
Fig. 5. Ray path geometry for Band-1 and Band-2 directions. ABCD is the crack plane of parallel vertical cracks. S is the recorder position on a horizontal free-surface. Band-1 directions to the horizontal free-surface, where time-delays are sensitive to crack aspect-ratios. are those within the solid angle EFGHS subtending 15° to 45° to the crack plane (within the effective shear-wave window). Band-2 directions to the horizontal free-surface, where time-delays are dominated by crack densities, are those within the solid angle ADEHGS subtending 0° to 15° to the crack plane. Both Band-1 and Band-2 directions include the equivalent solid angles reflected in the other side of the imaged crack plane.

3.4. The ±80% scatter in time-delays above small earthquakes

Above small earthquakes, time-delays typically display a ±80% scatter [45]. This cannot be explained by conventional geophysics [46], but the scatter, and the occasionally observed 90°-flips in shear-wave polarisations above large faults, can be modelled by 90°-flips associated with the critically-high pore-fluid pressures expected on all seismically-active faults [45] as a consequence of the New Geophysics [10,11,92]. 90°-flips near a fault-plane result in 'negative' time-delays. Surface observations are a combination of a negative time-delays near a fault, and positive time-delays in the normally pressurised remainder of the ray path to the surface. With a large fault the negative delays associated with the 'flipped' polarisations dominate the polarisations and may be observed at the surface [44]. However, for the majority of earthquakes on smaller deeper faults, the 'positive' time-delays of the normally pressured path to the surface dominate, and typical stress-aligned polarisations are observed at the surface. The modelling of Crampin et al. [45] shows that small differences in the ratio of the length of 'flipped' to of the length of the normally pressurised ray paths can easily lead to the ±80% scatter in time-delays observed at the surface. These phenomena require the compliance of microcracks rather than the stiffness of macro-cracks to cause variations of shear-wave splitting.

3.5. The sensitivity of Band-1 time-delays

The sensitivity of Band-1 time-delays allows the stress-accumulation before large earthquakes to be identified if there are sufficient shear-wave arrivals in Band-1 directions in the shear-wave window above a swarm of small earthquakes. The average time-delays are observed to increase until a level of fracture-criticality is reached, typically between 4 [27] and 18 ms/km [5] depending on the particular stress and heat-flow regime, when the impending earthquake occurs. The logarithm of duration of the increase is observed to be proportional to the magnitude of the earthquake (Fig. 7a). Shear-wave splitting has been observed in records of natural and induced events with frequencies from 0.5 Hz [97] to mHz [98], but the more restricted data sets where temporal changes have been observed before larger earthquakes are typically from 10 Hz to 20 Hz [5].

Whenever appropriate source-recorder geometry exists, with sufficient observations in Band-1 directions near a large earthquake or some other change in *in situ* stress, changes in shear-wave splitting above small
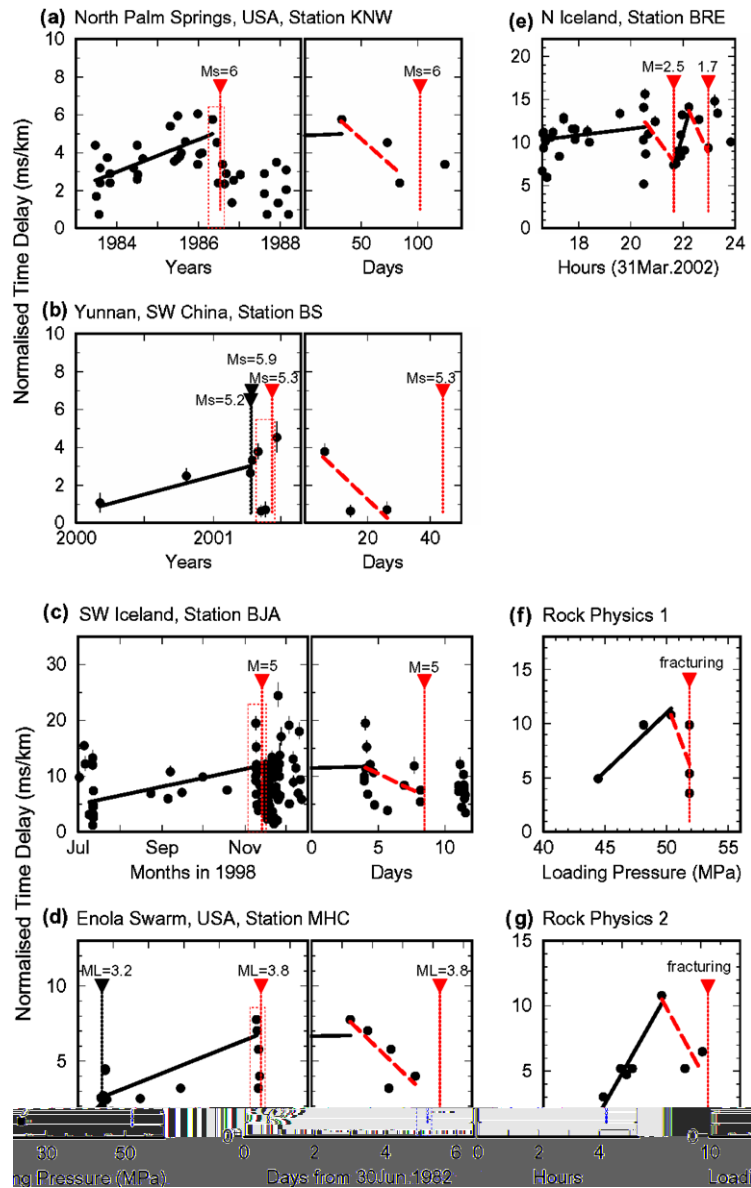
Fig. 6. Increases and decreases in time-delays observed in both field and laboratory. Temporal variations of shear-wave time-delays normalised to ms/km before earthquakes and laboratory experiments plotted against time duration for earthquakes and increments of applied stress for laboratory. (a) *Ms* 6 North Palm Springs Earthquake [23]. Left-hand-side: time-delays with a least-squares line showing increase for 3 years before the earthquake. Right-hand-side: enlarged time scale for dotted box in left-hand-side, with dashed line showing precursory decrease in time-delays starting 68 days before the earthquake. (b) *Ms* 5.3 earthquake (the last of three closely-spaced *Ms* 5+ earthquakes) in Shidian, Yunnan, China [6,22]. Notation as above with poorly resolved increase before the *Ms* 5.9 earthquake, but precursory decrease of 38 days before the *Ms* 5.3 earthquake. (c) *M* 5 earthquake in SW Iceland [21]: with increase for 5 months and precursory decrease of 4.4 days. This earthquake was stress-forecast [21]. (d) *M*$_L$ 3.8 Enola Swarm event [6,18]: Notation as in (a) with increase for 4.1 days and precursory decrease of 3.5 hours. (e) *M* 2.5 and *Ms* 1.7 earthquakes in a swarm beneath Flatey Island. Northern Iceland [6] with increases for 5.0 and 1.3 h, respectively, and precursory decreases of 1.12 and 0.73 h, respectively. (f and g) Variation in time-delays in two samples of marble, subjected to uniaxial stress increments until fracturing and fragmentation, for ray paths perpendicular to uniaxial stress [6]. The time-delays vary with time before spontaneous fracturing. (After [6].)

earthquakes have always been identified (summarised in Table 1). We do not claim that all aligned shear-wave splitting is necessarily caused by aligned cracks. Clearly, aligned crystals may cause splitting, but we know of no wholly authenticated observations of azimuthally-aligned shear-wave splitting along wholly crustal ray
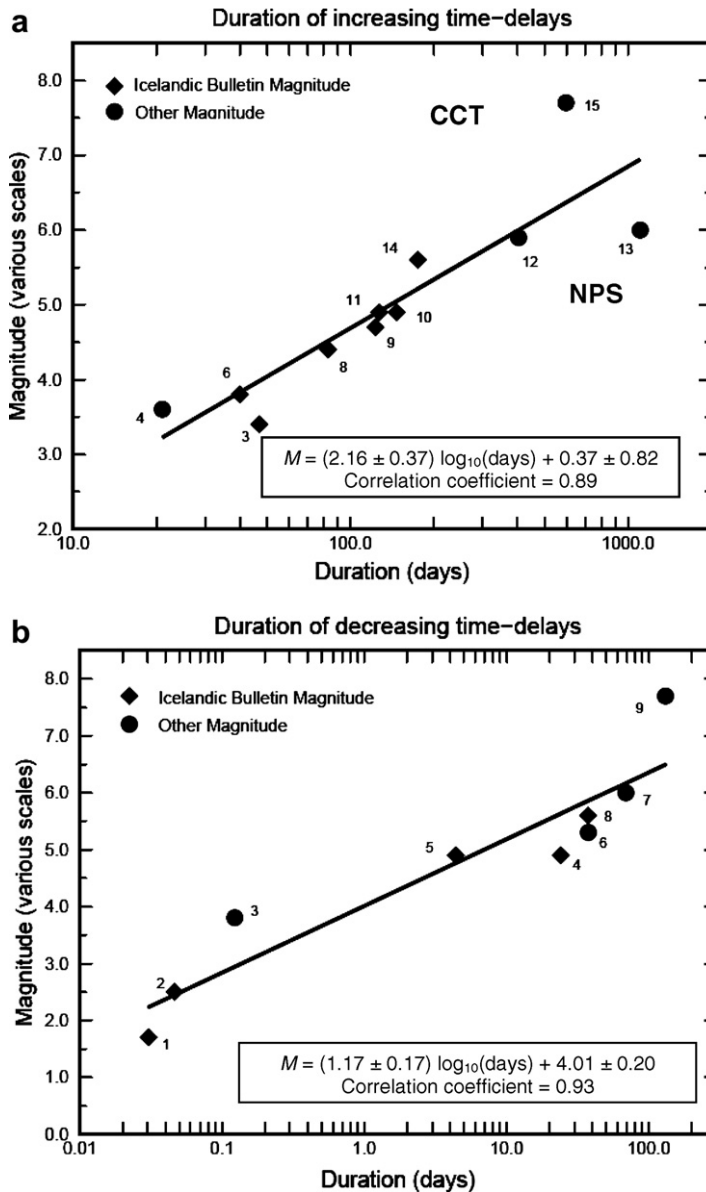
Fig. 7. (a) Logarithmic duration–magnitude relationship for the increases in time-delays (interpreted as stress-accumulation) for the earthquakes listed in Table 1a [20], omitting four earthquakes with questionable durations due to overlays with other earthquakes. (b) Logarithmic duration–magnitude relationship for the decrease in time-delays (interpreted as crack coalescence) for earthquakes listed in Table 1b [20]. The earthquakes labelled NPS and CCT refer to the 1988 *Ms* 6 North Palm Springs Earthquake, California, and the 1999 *Ms* 7.7 Chi–Chi Earthquake, Taiwan, respectively, which may well be subject to different rates of strain/stress increase than other earthquakes [20].

paths due to crystalline anisotropy. Fluid-saturated stress-aligned cracks must be the default interpretation. We also do not claim that azimuthally-aligned shear-wave splitting is invariably caused by *microcracks* (grain-boundary cracks and preferentially oriented pores) rather than *macro-cracks* with dimensions in tens of centimetres to tens of metres, say. There is also some controversy over the dimensions of cracks causing the splitting. However, heavily fractured beds with large cracks tend to severely attenuate the slower split shear-waves so that they are difficult to observe [14]. Equally, typical examples of microcrack-induced shear-wave splitting, as seen almost universally elsewhere, are also seen in rocks without significant visible fractures [98].

Table 4
Common fallacies in measuring and interpreting azimuthally-aligned shear-wave splitting above small earthquakes

	Fallacies	Summary[a] of preferred interpretation	Ref.
[F1]	Polarisations of split shear-waves are orthogonal.	Shear-waves propagating along seismic rays at the group velocity have polarisations which are not strictly orthogonal except in a few specific symmetry directions. Body-wave polarisations are orthogonal in all phase-velocity directions, but phase-velocity propagation is difficult to observe.	[1,7]
[F2]	Polarisations of split shear-waves are fixed, parallel to cracks, or normal to spreading centres.	Polarisations of shear-wave splitting always vary (three-dimensionally) with azimuth and incidence within the shear-wave window, even when propagating through parallel cracks, or normal to spreading centres.	[1,7,11]
[F3]	There is the same percentage of shear-wave velocity anisotropy in all directions, through any given set of parallel cracks, or through upper-mantle anisotropy.	Percentage of shear-wave velocity anisotropy always varies (three-dimensionally) with azimuth and incidence angle. When propagating through parallel cracks, or parallel to spreading centres, percentages may vary from positive to negative, within the shear-wave window. (Time-delays become negative when faster and slower split shear-waves exchange polarisations.) These may lead to very low or negative time-delays in some directions of propagation, and maximal values in other directions separated by as little as 30°.	[1,7]
[F4]	Polarisations observed at the free-surface are the polarisations along the ray path.	Incident polarisations are wholly preserved for surface observations only at normal incidence to a horizontal free-surface. Polarisations and orthogonality may be seriously disturbed at all other angles of incidence, where horizontal observations are projections of original polarisations onto the horizontal plane.	[1,7]
[F5]	Temporal changes in shear-wave splitting, caused by any plausible stress-induced changes in crack geometry, cause changes in time-delays for all ray paths within the shear-wave window.	Small changes in low-level stress are only likely to affect crack aspect-ratios, which will change the *average* time-delay in Band-1[b] directions of the shear-wave window (values may be positive or negative in particular directions within Band-1). Band-1 has mostly positive, say, time-delays but has a small solid angle of negative time-delays, so that averages need to be taken to measure overall variations in amplitude. Only large changes in stress will change crack density and modify time-delays in Band-2.	[7,11]
[F6]	The shear-wave window, in which shear-waves can be observed at the free-surface undistorted by *S*-to-*P* conversions, is aligned normal to the horizontal plane.	The shear-wave window is normal to the *free-surface* within about a wavelength of the seismic recorder. Since earthquakes are typically beneath irregular surface- (and subsurface-) topography, shear-wave splitting observed above small earthquakes may be severely distorted even within the nominal shear-wave window. Irregular topography may seriously modify shear-wave polarisations but has less effect on time-delays.	[80,81]
[F7]	Large percentages of crack-induced shear-wave velocity anisotropy, exceeding 5%, are possible.	Assuming crack-induced anisotropy (as we must for azimuthally-aligned shear-wave splitting; see Table 2, particularly [R1, R2]), only shear-wave velocity anisotropy in the range 1.5% to 4.5% (crack densities 0.015 to 0.045) is permissible in ostensibly intact rock. Higher crack densities imply such disaggregated rock that the slower split shear-wave is likely to be highly attenuated and probably unobservable [14]. Note, however, that higher levels of shear-wave velocity anisotropy are found in areas of high heat-flow in Iceland and near volcanoes. The cause of these high values is not yet fully understood.	[7,41,42]
[F8]	Shear-wave splitting observed at the free-surface is confined to the uppermost few kilometres.	Assuming crack-induced anisotropy, confining the anisotropy to the near-surface often would imply impossibly-high crack densities [F7]. Although there may be higher crack-induced anisotropy near the surface, there appears to be pervasive shear-wave splitting throughout most levels of the crust. *Saiga [104], observed shear-wave splitting down to 30 km in Tokai, Japan, and *Gledhill [54] observed uniform shear-wave splitting down to 34.8 km in Wellington Peninsular, New Zealand.	[7]

Table 4 (continued)

	Fallacies	Summary[a] of preferred interpretation	Ref.
[F9]	The scatter in time-delays and polarisations observed at station networks implies anisotropy confined to near-surface layers.	The large ±80% scatter in time-delays and polarisations invariably observed above small earthquakes is caused by the sensitivity of shear-wave splitting to the critically-high pore-fluid pressures on all seismically active fault-planes. Without clear direct evidence of shallow anisotropy, observed scatter does not imply near-surface anisotropy. See also [F7] and [F8].	[44,45]
[F10]	Lack of correlation of time-delays with epicentral distance or depth indicates that the anisotropy is confined to the near-surface.	The large ±80% scatter [F9] and the theoretical variation of time-delays in Band-1 [F5] frequently hide correlations of time-delays with distance or depth, except for very substantial data sets, when averages are meaningful.	[7,42,44,45]
[F11]	Temporal variations in (normalised) time-delays can only be compared along nearly identical ray paths.	Even along identical ray paths above small earthquakes, rapid localised changes in pore-fluid pressure are likely to cause (seemingly) random fluctuations in cumulative delays, so that a large data set of arrivals, well distributed in time, is necessary to detect overall temporal changes. Two or three arrivals from the same ray path are not sufficient to demonstrate the presence or absence of temporal change, even if they are from events with apparently similar waveforms. The large scatter in time-delays [F9] means that only average values (in Band-1, say) can be compared and variations for different ray paths are hidden: also see [F10].	[7,44,45]
[F12]	90°-flips in polarisations are caused by orthogonal *shear-induced* fractures near faults.	APE-modelling shows that critically-high pore-fluid pressures cause fault-parallel cracks rather than cracks oriented by regional stress. It is these fault-parallel fractures which result in 90°-flips in shear-wave polarisations. APE models the mechanism for inducing fault-parallel fractures.	[7,44,45]
[F13]	Crack anisotropy always decreases with depth as fluid-filled cracks are closed by lithostatic pressure.	Fluid-filled cracks are only closed by pressure if the fluid is removed by chemical absorption, drainage into sinks at depth, or by dispersion or flow towards the surface. The amount of chemical absorption is limited, pressure sinks at depth are rare, crystalline rocks usually have low permeability, and impermeable seals are common above sedimentary oil reservoirs. The presence of fluids (and hence fluid-saturated cracks at all depths) is confirmed by deep oil reservoirs, fluids at 12-km depth in the Kola deep well, and by high conductivity in the lower crust, also see [F7, F8].	[93,94,106,107]
[F14]	Interpreting the lack of observed temporal changes in shear-wave splitting during aftershock sequences as evidence that shear-wave splitting does not vary with earthquakes.	During sequences of aftershocks, stress distributions undergo fluctuating disturbances as stress is repeatedly released by earthquakes, with foci typically alternating between ends of the fault. This means that fluid-saturated microcrack geometry is likely to be sporadic and irregular. Consequently, consistent variations of shear-wave splitting are not expected and have not been recognised during aftershock sequences. In addition, aftershock sequences typically release a very small percentage of the energy of the main shock so any stress-induced anomalies thereafter are likely to be small.	
[F15]	Signal-to-noise ratios of shear-wave splitting above small earthquakes can be improved by stacking.	As time-delays and polarisations each vary with both incidence angle and azimuth of propagation [F2, F3, F9, F12], stacking arrivals from similar or different ray paths above small earthquakes invariable degrades the consistency of the signal and decreases signal-to-noise ratios. Only with a controlled source is stacking useful.	[1,7]

Table 4 (*continued*)

	Fallacies	Summary[a] of preferred interpretation	Ref.
[F16]	Plotting maps of polarisations at epicentral locations rather than observing seismic station.	Since time-delays and polarisations vary with both incidence angle and azimuth of propagation [F2, F3], maps of these parameters plotted at epicentres (or halfway to the epicentre) may be misleading as they do not convey consistent three-dimensional information. Plotting polar projections of variations at seismic stations is believed to be meaningful and is at least an actual observable.	[1,7]
[F17]	Use cross-correlations as the main technique to show presence or absence of temporal changes in shear-wave splitting.	Temporal changes in shear-wave splitting are typically so small (typically less than 0.2 s, usually substantially less) that it usually impossible to define a suitable cross-correlation window small enough, on large-amplitude irregular seismograms, to be sensitive to a small differential changes.	[25,59]

References to items in this table will be cited as [F?].
[a] The summarised interpretations are expanded in the cited references.
[b] Band-1 and Band-2 are specified in the last paragraph of Section 3.

4. Common fallacies about shear-wave splitting

Undisturbed *in situ* rock is totally inaccessible below the uppermost few metres. Boreholes penetrating deeper rock seriously disturb the surroundings, by stress release, temperature anomalies, and fluid invasion, to at least six times the borehole radius [98], and certainly much further. Consequently, behaviour in boreholes, as seen by borehole televiewers, sonic or dipole logs, and other logging devices, is not representative of conditions in the intact undisturbed rock mass many diameters away from the well. Hence, the true behaviour of compliant fluid-saturated *in situ* microcracks is difficult to ascertain and easy to misinterpret. It is also easy to make judgments about shear-wave splitting at one location, cherry-picking evidence, without taking into account the implications of the overall evidence, which we try to present in this review (Table 2). These are currently areas of apparent controversy, which this review hopes to resolve.

Table 4 lists some 17 common fallacies about shear-wave splitting. Note that our understanding of shear-wave splitting has recently advanced substantially and some of the listed fallacies have only recently become apparent. In the Appendices, we discuss a range of further papers, in addition to the five in Table 3, many of which were published before all the listed fallacies were recognised. Consequently, the interpretation of many of these papers was based on an earlier less-complete understanding of shear-wave splitting, and some of the earlier interpretations can now be discounted. We particularly comment on papers relating to compliant stress-aligned fluid-saturated microcracks showing temporal variations in shear-wave splitting, which directly indicate critical-systems of fluid-saturated stress-aligned microcracks.

5. Review of observations of temporally-varying shear-wave splitting

There are now probably well over fifty publications observing and interpreting azimuthally-aligned shear-wave splitting above small earthquakes. These are far too many to review individually, and we shall review only to a few "type" examples, particularly those which display temporal variations in shear-wave splitting, that we suggest are key papers for the interpretation of shear-wave splitting. In view of what we suggest is irrefutable evidence for stress-aligned fluid-saturated microcracks as the dominant cause of shear-wave splitting listed in Section 2.1 and Table 2, we concentrate on demonstrating how the fallacies listed in Table 4, have led to misinterpretation of the cause and distribution of shear-wave velocity anisotropy and fluid-saturated microcracks.

The typical temporal variations before earthquakes are that the increase in the average shear-wave time-delays (in Band-1 of the shear-wave window, sensitive to changes of stress) is *self-similar* with the earthquake magnitude (the logarithm of the duration of the increase is proportional to the magnitude of the impending event [5]) as shown in Fig. 7a. This is believed to monitor stress-accumulation before the earthquake. In

addition, in all cases where there is sufficient data to show the phenomenon, the increase in time-delays abruptly begins to decrease shortly before the earthquake [6], where the logarithm of the duration of the decrease is again self-similar to the magnitude of the impending event as shown in Fig. 7b. This stress relaxation is believed to monitor crack coalescence before the actual fault break. Fifteen earthquakes where increases have been seen are listed in Table 1a. Of these, nine, where there were sufficient source events, also show precursory decreases (Table 1b). We refer to these increases and decreases as *classic* examples of self-similar time-delay variations before earthquakes. Fig. 6 shows typical examples of increases and precursory decreases in Band-1 time-delays for seven earthquakes and two laboratory stress cells.

There have been extensive studies in two regions: California, where temporal variations in shear-wave splitting before earthquakes were first identified; and Iceland, where recent studies form the background to much of our current understanding of shear-wave splitting. Observations and interpretations of shear-wave splitting including those where classic temporal variations before earthquakes have been observed are summarised in Appendices: (A) California; (B) Iceland; and (C) elsewhere. We also add Appendix D): temporal changes in shear-wave splitting observed before, during, and after volcanic eruptions, and Appendix E): temporal changes in shear-wave splitting observed during other phenomena.

For convenience, throughout the appendices and the reference list, papers reporting shear-wave splitting where temporal variations have been recognised, either by the authors or by our re-interpretations, have the citation and reference marked by an asterisk '∗'. The section heading for each paper discussed in the appendices will include those crack properties [R?] (Table 2) and/or fallacies [F?] (Table 4) most relevant to the particular paper or papers. Note that papers published on data from Iceland, Italy, and China, have generally known and avoided the fallacies listed in Table 2.

6. Summaries of appendices

6.1. Temporal changes in shear-wave splitting before earthquakes in California

Appendix A cites more than ten papers referring to observations of shear-wave splitting in California, where temporal variations were first identified. These various observations, when examined in the context of worldwide observations of shear-wave splitting, are without exception consistent with distributions of compliant stress-aligned fluid-saturated microcracks pervading the crust. The classic self-similar temporal variations of increases and decreases in Band-1 time-delays are seen before two earthquakes, the M_S 6, 1986, North Palm Springs Earthquake [6,27–29], and a M_L 4, 1989, Parkfield Earthquake [23]. Other less classic examples of temporal changes are also seen above small earthquakes in the Los Angeles Basin [99] and in various analyses above earthquakes observed by the seismic network of Parkfield Earthquake Prediction Project [100,101].

6.2. Temporal changes in shear-wave splitting before earthquakes in Iceland

Appendix B briefly outlines the extensive observations of shear-wave splitting in Iceland, where much of the current understanding of shear-wave splitting was first established. Iceland has persistent swarm-type seismicity associated with transform faults of the Mid-Atlantic Ridge which unusually run onshore and provide ideal sources for studying shear-wave splitting within the shear-wave window above the source. Classic stress-accumulation increases have been identified in retrospect before some eight earthquakes in Iceland [5,6,24,30] and one M 5 earthquake was successfully stress-forecast in real-time [25] (Table 1). It is likely that had the improved seismic catalogue (with magnitudes down to M 0 and below) been available at the time, the pair of Ms ∼6.6, June 2001, earthquakes, the largest in Iceland for some decades, would also have been stress-forecast in real time [30]. Iceland is highly active tectonically, and shear-wave splitting time-delays have been shown to be sensitive to changes in stress due to magmatic as well as seismic activity. Small magmatic episodes disrupt the classic variations in time-delays before earthquakes, except for long duration increases before larger earthquakes, short duration increases before very small earthquakes, and during the 2-year stress adjustment following the large Vatnajökull eruption when minor magmatic disturbances were absent [5].

6.3. Temporal changes in shear-wave splitting before earthquakes elsewhere

Appendix C reports that temporal changes in shear-wave splitting time-delays before earthquakes are a widespread phenomenon that has been observed in a variety of different regions worldwide. Classic examples of temporal changes in shear-wave splitting before earthquakes have been observed in: Arkansas, USA; two areas in China; two areas in Italy; and probably before distant earthquakes near the Wellington Peninsula, New Zealand. There are no contrary observations where adequate source earthquakes have not shown variations in time-delays before larger earthquakes.

There are several studies from New Zealand, Gledhill [54,102] and Balfour et al. [103], where the shear-wave splitting has complicated polarisations, almost certainly caused by the severe topographic irregularities in both locations. Gledhill and Balfour et al. did not find evidence for temporal changes. This was at least partly because the significance of Band-1 and Band-2 directions had not been established when Gledhill's measurements were originally made. However, Gledhill's data may show both increases and precursory decreases before distant offshore earthquakes.

6.4. Temporal changes in shear- wave splitting before volcanic eruptions

Appendix D reports temporal changes in shear-wave splitting time-delays before three volcanic eruptions. The 1996, Gjàlp eruption, in the Vatnajökull Ice Field, in Iceland showed increases in Band-1 time-delays at ∼240-km distance in three directions (Table 1c). Gjàlp did not show a precursory decrease, but following the eruption the time-delays showed a gradual decrease over about 2 years [5]. Bianco et al. [32] report several 90°-flips in shear-wave polarisations before a flank eruption on Mt. Etna which also showed precursory decreases immediately before the eruption. The interesting feature of this behaviour is that the increase in time-delays and the precursory decrease is very similar to the classic increase and decrease in Band-1 time-delays observed by Del Pezzo et al. [104] before an earthquake on Mt. Vesuvius. Miller and Savage [33] report 90°-flips in shear-wave polarisations at Mt. Ruapehu, New Zealand, which they attribute to the effects of high-pressures before magma erupts at the surface, and speculate that eruptions can be predicted by such behaviour [47].

Clearly, more observations of temporal variations in shear-wave splitting before eruptions are needed to determine whether both the stress-accumulation increase and the precursory decrease in time-delays are universal for all eruptions, as they appear to be for all earthquakes. There is a wide variety of different types of eruption and it is possible that shear-wave splitting may show behaviour distinguishing types of eruption.

6.5. Other observations of temporal variations in shear-wave splitting

Appendix E reports six other examples of temporal changes in shear-wave splitting. Angerer et al. [35] use APE to successfully model the response of a fractured carbonate reservoir to both high- and low-pressure CO_2-injections. This is the most direct *in situ* calibration of APE-modelling to-date and confirms the existence of critical-systems of fluid-saturated stress-aligned microcracks. Bokelmann and Harjes [36] report changes in shear-wave splitting following fluid-injection at 9-km depth in the KTB Fracture Experiment in SE Germany caused systematic changes in splitting at 4-km depth in the 190-m offset pilot well. Teanby et al. [37] report possible tidal variations in borehole observations of shear-wave splitting in production-induced events in the North Sea. Crampin et al. [38] report the SMSITES cross-hole seismic experiment in Iceland where well-recorded anomalies coincide with distant low-level seismic activity which indicates the great sensitivity of the crack-critical crust to minor disturbances. Crampin and Booth [39] report changes in polarisations of shear-wave splitting during hydraulic pumping in a hot-dry-rock experiment in Cornwall. In initial pumping tests, shear-wave polarisations were parallel to joints and fractures in outcrop rocks, whereas when hydraulic fracturing began, polarisations changed by ∼7° to became parallel to the measured direction of maximum horizontal stress. Tang et al. [40] report anomalies during fluid-injection near the Krafla volcano, Iceland, and in the Cocos Geothermal Field, California. The cause of these anomalies, see Section E2.6, is not understood but is believed to be due to local behaviour in the proximity of the injection points.

6.6. Overall summary

The appendices discuss some 30 reports of temporal changes in shear-wave splitting at some 20 different locations. Many of which are the classic variations of longer term increases in Band-1 shear-wave time-delays and shorter precursory decreases immediately before the impending events. There are no contrary observations, and we conclude that the immediate effect of low-level changes of stress on the rock mass, as in the stress-accumulation before earthquakes or the inferred crack coalescence stress relaxations, is to modify microcrack geometry that can be monitored by shear-wave splitting.

7. Discussion

Since the interior of the Earth is largely inaccessible it is difficult to directly prove even the existence of fluid-saturated stress-aligned compliant microcracks at depth in the crust. The arguments in Table 2 [especially R1] and Section 2 that parallel shear-wave splitting polarisations imply TIH-anisotropy, and that stress-aligned vertical cracks are the only cause of TIH common to almost all rocks, are diagnostic and compelling, but technical. The most direct demonstrations of *in situ* cracks are: (1) fluid-saturated microcracks are the only immediately compliant element of *in situ* rocks; and (2) since shear-wave splitting monitors microcrack geometry, the observed short-term temporal variations in shear-wave splitting necessarily imply distributions of fluid-saturated microcracks. This raises the question of whether we can distinguish between temporal and spatial variations, and whether the anisotropy is shallow or deep in the crust.

7.1. Temporal versus spatial variations of shear-wave splitting?

The appendices report changes in shear-wave time-delays before 15 earthquakes, before three volcanic eruptions, and changes during six other investigations. A crucial question is whether these changes are due to *temporal* variations in shear-wave splitting caused by stress-induced changes to microcrack geometry as suggested above, or whether the changes are caused by *spatial* migration of shear-wave source events, as suggested by Liu et al. [50,56].

The locations of swarms of earthquakes used as the shear-wave source events are seldom wholly random distributed and sometimes display migration of foci with time. However, the effect of changes of source location on measurements of time-delays to seismic stations is difficult to evaluate because, even in a wholly uniform stable anisotropic structure, the degree of seismic anisotropy varies with direction of propagation in three dimensions, as well as varying temporally as the local stress-field is modified by every small earthquake [45].

Enlarging on the arguments summarised in Table 2, we discuss evidence for changes being temporal variations in anisotropy rather than spatial variations in shear-wave source events.

(1) All 15 earthquakes (Table 1a), where temporal changes have been observed, show similar variations with a long-term increase of normalised time-delays (in Band-1 of the shear-wave window) before larger earthquakes, which can be modelled as stress-accumulation [7].
(2) Whenever there are sufficient source events (nine cases out of 15, Table 1b), the normalised time-delays also display a precursory decrease immediately before the larger earthquake. Fig. 6 shows six examples of increases and precursory decreases scaled with time.
(3) The logarithms of durations of both increases and decreases are self-similar with the magnitude of the impending earthquakes [5,6,24,30].

For the effects of source migration to give characteristic self-similar patterns of systematic behaviour in 15 different source zones (Table 1) along paths to arbitrary distributions of seismic stations (as in Fig. 6) would be extremely unlikely coincidences. We conclude that the observations of temporal variations in shear-wave splitting are monitoring (at least partially understood) *temporal* variations in microcrack geometry.

Two controlled source experiments directly confirm temporal changes in shear-wave splitting and hence of the compliance of fluid-saturated microcracks. Angerer et al. [35] (Section E2.1) used APE to model the effects

of both high-pressure and low-pressure CO_2-injections on shear-wave splitting, and Crampin et al. [38] (Section E2.4) reported measurements of cross-hole seismics showing temporal variations of the rock mass responding to seismic release equivalent to a *M* 3.5 earthquake at an epicentral distance of ~70 km.

7.2. Shallow versus deep anisotropy?

Observations of azimuthally-aligned velocity variations and shear-wave splitting are always a combination of the anisotropy along the whole of the ray paths and do not directly identify the depth-range where the anisotropy occurs. Consequently, other information must be used to infer depths. The association of the anisotropy with stress-aligned microcracks (Table 2) imposes limits on depths. Since cracks are generally aligned perpendicular to the direction of minimum compressional stress, near the free-surface where the minimum stress is vertical, horizontal cracks may be expected in the uppermost 500–1500 m of the crust [5,7,43], and anomalous observations must be expected above these depths. Since observations of velocity variations and shear-wave splitting of TIH-anisotropy are consistently aligned with the direction of horizontal stress, whenever this can be identified or inferred, stress-aligned anisotropy is indicated below 500–1500 m worldwide. Observations suggest that such stress-aligned anisotropy is uniformly distributed below such depths throughout at least the upper half of the crust.

Several of the papers reviewed in the appendices argue that, because shear-wave time-delays and polarisations change rapidly between neighbouring seismic stations, and because the time-delays do not uniformly increase with length of ray path, the anisotropy is necessarily confined to the near-surface. It is difficult to evaluate the depth-range because observed shear-wave time-delays are the cumulative sum of the time-delays along the whole of the ray path (assuming similar anisotropic orientations, as is often the case). Any observed time-delay may be caused by stronger anisotropy at either end of the ray path, or by uniform but weaker anisotropy along the whole length of the ray path. There are two main causes of variations in surface observations: (1) shear-waves have strong reactions with surface topography, so that irregular topography modifies the effective slope of the free-surface in the shear-wave window. Most small earthquakes, and hence most shear-wave source events, tend to be in hilly and mountainous areas, where the slope around the seismic recorder may seriously modify observed shear-wave polarisations; and (2) the scatter in time-delays caused by high-pressure-induced 90°-flips in shear-wave polarisations above small earthquakes introduces a ±80% scatter in observations of time-delays [45]. This means that shear-wave time-delays are heavily scattered. Consequently, variations in time-delays are only statistically valid in averages of substantial data sets, and substantial data sets of seismic data *before* larger earthquakes are scarce, with perhaps only one wholly adequate statistically valid example to-date [27]. However, in all cases where there are sufficient source events (Table 1a and 1b), despite the scatter least-squares averages indicate stress-accumulation increases, and crack coalescence decreases. In addition, concentrations of anisotropy in the near-surface would typically lead to unacceptably high crack densities. Arguments for the preferred interpretation of similar anisotropy along the whole of the ray path are summarised in Table 4 in fallacies [F6, F8, F9, F10].

Japan and New Zealand have both shallow and intermediate depth earthquakes which allow specification of the depth-ranges for anisotropy. *Saiga et al. [105] observed consistent shear-wave splitting down to 30 km in the Tokai region, Honshu, Japan. *Gledhill [54] found consistent shear-wave splitting throughout the crust down to 35 km. Elsewhere, both Graham and Crampin [106] in Turkey, and Yegorkina et al. [107] in Armenia, observed consistent polarisations of shear-wave splitting throughout the whole thickness of the crust from shear-waves from regional earthquakes refracted from the Moho estimated as 29-km deep in Turkey, and a notional 33-km deep in Armenia. In both cases, shear-wave time-delays of 1 s or more throughout the crust imply anisotropy of the lower crust at least twice as strong as in the upper crust.

A comprehensive *P*-wave refraction experiment beneath Mount Hood, Oregon [108] provides information about possible crack fluid content at depth [109]. The *P*-wave anisotropic velocity variations could be interpreted in terms of stress-aligned fluid-filled cracks filled with, successively from the surface: liquid water; super-critical water [110]; and fluid melt. Equating temperatures beneath Mount Hood with equivalent temperatures elsewhere in the crust suggests that shear-wave splitting in the lower half of the crust is, at least partially, due to cracks filled with super-critical water which has temperature- and pressure-sensitive acoustic velocities [109]. Cracks filled with super-critical water in high-temperature regimes in the crust is the probable

Table 5
Arguments for aligned melt-filled cracks as the cause of upper-mantle shear-wave splitting (After [111])

	Observations in upper-mantle	Interpretation
1	Fast shear-waves aligned parallel to stress/fluid-flow for a polar window to at least 30° incidence.	This is the symmetry of vertical parallel cracks aligned parallel to stress directions. Crystalline anisotropy does not usually result in parallel polarisations over such a wide angle of symmetry [1].
2	Shear-wave velocity anisotropy of typically 1% to 5%.	1% to 5% is the typical velocity anisotropy of cracks in intact rock in the crust [2]. Crystalline anisotropy of upper-mantle constituents may have shear-wave velocity anisotropy of up to more than 30% depending on crystal type and purity. Hence crack anisotropy is appropriate to the upper-mantle [1].
3	As Items 1 and 2, above.	As crystals approach melting temperatures, melting begins along grain-boundaries, leading to distributions of liquid (hydrated) melt-filled films along grain boundaries, analogous to liquid (water) filled microcracks in the crust.
4	Time-term anisotropy analysis of *P*-wave reflection/refraction surveys around the high-temperature crust beneath Mount Hood, Oregon, USA [108].	Anisotropy analysis yields *P*-wave velocity variations suggesting that stress-aligned cracks are filled with liquid (water) at 1-km depth; super-critical fluid (water) [110] at 3.7-km depth; and liquid melt-filled cracks below 8.5 km, implying aligned melt-filled cracks in the upper-mantle [109]. Equating high temperatures beneath Mount Hood to equivalent crustal temperatures suggests that the lower crust is pervaded by cracks containing super-critical water, and the upper-mantle by cracks containing (hydrated) melt [109].
5	Mechanisms of earthquakes in the mantle generally appear to be similar to those of crustal earthquakes	Since it is commonly argued that earthquake mechanisms in the crust are largely controlled by fluids as in microcrack deformation [41,42], it is highly likely that earthquakes in the mantle are also controlled by the deformation of fluid-saturated cracks.
6	As Items 1, 2, and 3, above.	Items 1, 2, and 3 suggest that the crust is a critical-system of fluid-saturated microcracks. The universality of critical-systems (one of the properties of critical-systems [17–19]) suggests that they apply over all available space, that is all fluid-saturated rocks [10,38,42]. Since the upper-mantle contains cracks filled with hydrated melt, the universality of critical-systems suggest the cause of the shear-wave splitting is aligned fluid-filled cracks in the upper-mantle.

explanation of the high time-delays seen in Iceland. In most regions of the crust without high heat-flow, nor-malised levels of fracture-criticality when rocks fracture, are between 4 and 8 ms/km [7,27], whereas in Iceland, where heat-flow is high, fracture-criticality is typically between 10 and 18 ms/km [5].

The interpretation of melt-filled cracks at depth beneath Mount Hood suggests that cracks or microcracks filled with films of hydrated melt would explain many features of shear-wave splitting observed in the mantle from various core phase arrivals [111]. Table 5 summarises the evidence for crack-induced anisotropy in the upper-mantle.

8. Conclusions

Table 2, particularly [R1], suggests that distributions of stress-aligned fluid-saturated microcracks are the predominant cause of the nearly universal observations of azimuthally-aligned shear-wave splitting both in the Earth's crust, and arguably in the upper-mantle (Table 5). The various appendices, together with APE-modelling, support the hypothesis that the stress-aligned fluid-saturated grain-boundary cracks in crystalline rocks and preferentially oriented pores and pore throats in sedimentary rocks are the most compliant elements of *in situ* rocks, so that changes of stress before earthquake will systematically modify shear-wave splitting before larger earthquakes. The appendices confirm that shear-wave splitting monitors the deformation of

microcracks and shows systematic changes before impending earthquakes. The precision of controlled source observations (Sections E2.1 and E2.4), as opposed to the scatter associated with earthquake sources, indicates that cross-hole seismics in borehole stress-monitoring sites (SMSs) can monitor the accumulation of stress before impending earthquakes and estimate the time, magnitude, and estimated location of impending large earthquakes (see Section E2.4). Although the quality of the various data sets varies widely, there are no contrary events where appropriate data do not show temporal changes before large earthquakes.

This means that in principle, cross-hole seismics at appropriate directions and depths can monitor the build-up and precursory decrease of stress before earthquakes and stress-forecast the time and magnitude of the impending event where other precursory phenomena indicate the approximate location.

Finally, as an aside, it is fortunate for geoscientists that the observed pattern of shear-wave splitting polarisations in the Earth are typically oriented either parallel, the result of TIH-anisotropy, or radial, the result of TIV-anisotropy Hexagonal symmetry (transverse isotropy) in these two orientations is a particularly simple easily-specified easily-understood symmetry system. All other anisotropic symmetry systems with the third polarisation pattern are much more complicated and would be much harder to interpret and exploit.

Acknowledgement

Appendix A. Temporal changes in shear-wave splitting before earthquakes in California (Appendix A is summarised in Section 6.1.)

Note that throughout the appendices and reference list, papers where temporal changes in shear-wave splitting have been recognised, either by the original authors or by our re-interpretations, are marked by '*'.

A.1. Introduction

*Peacock et al. [27] and *Crampin et al. [28] measured shear-wave time-delays in polarisation diagrams at Station KNW of the Anza Seismic Network, Southern California, before the *Ms* 6, 1986, North Palm Springs Earthquake, ~30 km from KNW, and were the first to identify temporal variations in shear-wave splitting before earthquakes. The variations in polar projections of time-delays were attributed to increases in crack aspect-ratios in distributions of stress-aligned fluid-saturated microcrack, as strain accumulated (now referred to as 'stress-accumulation') for 3 years before the earthquake. This behaviour, initially hypothetical, was theoretically confirmed when the anisotropic poro-elastic (APE) model of fluid-rock evolution was developed by Zatsepin and Crampin [41] and Crampin and Zatsepin [42]. (Later, *Gao and Crampin [6] also identified, on the same data set, an abrupt decrease in time-delays some 70 days before the onset of the earthquake.) The hypothesis for the sensitivity of shear-wave splitting to stress changes before earthquakes generated a number of papers by Aster, Shearer, Fletcher, and others reported in this Appendix, investigating surface seismic and borehole evidence for distributions of fluid-saturated stress-aligned microcracks. This appendix will discuss key papers relevant to temporal variations of shear-wave splitting in California in chronological order.

A.2. Observations and interpretations of shear-wave splitting

A.2.1. Aster et al. [57] (subject to fallacies: [F4, F8, F9, F10, F13, F17], Table 4)

Aster et al. [57] used an automatic technique to analyse shear-wave splitting in the same data set where *Peacock et al. [27] and *Crampin et al. [28,29] recognised temporal variations of time-delays before the 1986, *Ms* 6, North Palm Springs Earthquake in Southern California. However, no satisfactory wholly-automatic technique for measuring shear-wave splitting has yet been developed [59], and *Crampin et al. [29] showed that the automatic technique of [57] gave errors of up to 200% (factors of 3) in shear-wave time-delays. Such errors are so severe that results and conclusions based on these automatic evaluations of time-delays in

[57] can be discounted. The comment and response is summarised in Item 4 of Table 3. The misinterpretations of Aster et al. [57] may be attributed to fallacies [F4, F8, F9, F10, F13, F17] in Table 4.

A.2.2. Fletcher et al. [112] ([R1], Table 2. There are no notable fallacies.)

Fletcher et al. [112] studied near-surface site effects at two 300-m deep boreholes. One borehole, KNW-BH, was 391 m from the surface seismic station KNW near the San Jacinto Fault in Southern California, where *Peacock et al. [27] and *Crampin et al. [28] had observed temporal changes. Both KNW and KNW-BH are in areas of irregular surface topography. The other borehole (at Piñon Flat) did not record local earthquakes and is irrelevant to this discussion.

Conclusions of Fletcher et al. [112] relevant to this review.

(1) Deeper granitic rocks at KNW-BH are competent and have few obvious cracks or discontinuities, but near-surface structure at KNW-BH, particularly above 70-m depth, is highly disturbed. Fletcher et al. conclude that this is likely to complicate observations of shear-wave splitting at the surface, where high-frequencies from recordings of local earthquakes may mask the lower-frequency split shear-wave arrivals.

(2) Consequently, they suggest that interpretations using only particle motion diagrams (polarisation diagrams, PDs) as used by *Peacock et al. [27], and many papers by *Crampin et al., at single stations, are suspect as it is impossible to separate deep effects from local structure.

(3) Fletcher et al. also conclude that shear-wave splitting studies should concentrate on data sets where there are multiple arrivals from neighbouring stations (or borehole arrays) to identify the effects of near-surface interference.

Comments:

(1) Recognition of competent basement rocks agrees with the interpretations of *Peacock et al. [27] and *Crampin et al. [28,29], where the characteristic temporal variations they observed are now seen worldwide ([5,6,43,45], Table 1, and throughout this review). Surface observations of shear-wave splitting above small earthquakes typically have frequencies of 10–20 Hz with wavelengths of several hundred metres, and are unlikely to be heavily disturbed by the uppermost 70 m (unless the rock is wholly incompetent). However, near-surface interactions may contribute to the ±20° scatter in polarisations and the ±80% scatter in time-delays typically observed above small earthquakes [2,5,45] and high-frequencies could mask slower split shear-wave arrivals on seismograms as Fletcher et al. suggest. Abrupt changes of particle motion direction write characteristic signatures into PDs, and the uniformity of the observations of scatter, seen in a wide variety of source zones and surface conditions worldwide (Table 1), suggests that local conditions are not the primary source of the scatter. The effect of critically-high pore-fluid pressures on all seismogenic faults in a crack-critical crust is the preferred explanation of the scatter [45].

(2) The key diagnostic for identifying the arrival of both faster and, particularly, slower split shear-waves is the abrupt nearly-orthogonal change in particle motion direction which are most clearly seen in PDs (see discussion in Item 4 of Section 2.2). It is certainly true that shallow and deeper effects cannot be easily distinguished in PDs, but this is true of all measures of shear-wave splitting.

(3) It is certainly desirable to study shear-wave splitting at arrays of stations rather than single stations. Unfortunately, the geometrical source-to-recorder constraints on observing shear-wave arrivals within the shear-wave window, particularly with the need for large earthquakes to be nearby if temporal changes are to be investigated, are extremely constrained [7]. Consequently, there are few earthquake swarms and few individual earthquakes that are in the shear-wave window of more than one seismic station, and little progress would be made if studies of shear-wave splitting were restricted to multiple station observations.

Summary: The borehole observations of Fletcher et al. [112] are generally compatible with fluid-saturated stress-aligned microcracks causing shear-wave splitting.

A.2.3. Daley and McEvilly [113] [F3]

Daley and McEvilly [113] report a three-offset multi-azimuth VSP with orthogonal orientations of shear-wave vibrators to a permanently-installed string of three-component geophones to 1.4-km depth in the Varian Well of the Parkfield Earthquake Prediction Experiment on the San Andreas Fault, Southern California. This was intended to be the first of a series of repeated VSPs to monitor temporal changes in shear-wave splitting associated with what appeared to be a regular $\sim$20-year sequence of M 6 earthquakes at Parkfield. Unfortunately, the cable to the cemented geophones failed, so that the VSP study of Daley and McEvilly [113] could not be repeated. The anticipated M 6 earthquake did not occur until 28th September, 2004, some 12 years late. However Daley and McEvilly showed that the Varian VSP displayed clear near fault anisotropy which they assign to fluid-saturated cracks.

Conclusions of Daley and McEvilly [113] *relevant to this review*. Daley and McEvilly conclude that shear-wave splitting at Varian displayed TIH-anisotropy with a horizontal axis of symmetry perpendicular to San Andreas Fault. They found increasing time-delays as ray paths approach the vertical, which they interpret as implying more pronounced cracking in the stronger shear-fabric nearer the fault.

Comments. The polarisations and time-delays of the TIH-anisotropy observed at Varian are consistent with shear-wave splitting reported elsewhere in this review implying pervasive distributions of stress-aligned fluid-saturated microcracks. Note that in a uniform distribution of TIH-anisotropy, time-delays would theoretically increase as ray paths become closer to the vertical [7]

(2) The polarisations at KNW are N40°W, approximately fault-parallel, and the shear-wave splitting observed at KNW and the neighbouring borehole KNW-BH "most likely results from palaeo-strain mineral alignment … perhaps abetted by similarly aligned cracks near the surface … and that initial shear-wave particle motion directions do not necessarily indicate the present maximum compressive stress orientation".

(3) Aster and Shearer suggest that the 2.3 ± 1.7% shear-wave velocity anisotropy estimated for unweathered rock between 150 and 300 m can be accounted for by 3% per volume of aligned biotite crystals along the ray paths.

Comments:

(1) The shear-wave splitting at five of the Anza Stations is compatible with that caused by stress-aligned fluid-saturated microcracks as now observed extensively elsewhere.

(2) There are two phenomena that argue strongly against mineral alignment as the source of the anomalous polarisations at KNW (see Section 2.1 and Table 2). Anisotropy caused by mineral alignment does not typically lead to the near-parallel shear-wave polarisations within the shear-wave window indicative of TIH-anisotropy [R1] [1,7]. For mineral alignments to lead to the observed TIH-anisotropy, the minerals must have either hexagonal symmetry, or orthorhombic or other symmetry with mutual alignment along one axis but random orientation of the others. Furthermore, the axis of alignment would need to be horizontal and parallel to the slow shear-wave polarisation so that the perpendicularly polarised waves arrive first.Secondly, the anisotropies of mineral crystals typically have shear-wave velocity anisotropy much greater than the 1.5–5.5% shear-wave velocity anisotropy typically observed in most unfractured rocks in the crust [7] [F7]. Certainly, an unusual combination of minerals could lead to TIH-anisotropy with appropriate velocity anisotropy, but it would be an unusual and would be unlikely to lead to the almost universal observations of azimuthally-varying shear-wave splitting observed elsewhere.

(3) The elastic moduli of biotite (in the 3% per volume of biotite suggested by Aster and Shearer [116]) have exceptionally large ∼70% shear-wave velocity anisotropy (for pure biotite). For 3% biotite to be the cause the shear-wave splitting observed at KNW would require an exceptional coincidence: the proposed 3% mix of this highly anisotropic mineral with an isotropic matrix leading to the shear-wave velocity anisotropy of 1.5–5.5%, as observed by shear-wave splitting worldwide [2,5,7], would need to be stable throughout most of the crust. This seems unlikely.

Again the results of Aster and Shearer [116] are generally compatible with the compliant stress-aligned fluid-saturated cracks advocated in this review. Note that the fault-parallel shear-wave polarisations are some 40° from the directions of tectonic stress-aligned shear-wave polarisations observed at other stations of the Anza Seismic Network [27–29]. These can be attributed to the complicated effects of 90°-flips in shear-wave polarisations caused by the high pore-fluid pressures on all seismogenic faults [44,45]. Such polarisation anomalies can be observed at the surface near such major tectonic features as the San Andreas Fault in California and the Húsavík-Flatey Fault in Iceland, where major faults traverse most of the thickness of the crust [44]. At smaller faults the anomalies cause scatter in time-delays [45]. Fallacies [F7, F8, F9, F10, F12, F13] contribute to the misinterpretations of Aster and Shearer [116].

A.2.6. *Li et al. [99] [F9]

*Li et al. [99] examined shear-wave splitting above small earthquakes in the Los Angeles Basin. Assuming crack-induced anisotropy, they observed stress-aligned shear-wave splitting with the typical ±80% scatter observed elsewhere. Unfortunately, the time-delay data points are too sparse in time to show temporal variations before the several *M* 4 and *M* 5 earthquakes recorded during the observations, however there are enough source earthquakes to show that time-delays did decrease following a Montebello double-event, and then gradually rose to the average level. These observations are consistent with the presumed crack-induced observations seen elsewhere.

A.2.7. Zhang and Schwartz [117] [F2, F7, F8, F9, F10]

Zhang and Schwartz [117] examined shear-wave splitting above aftershocks of the 1989 Loma Prieta earthquake on a segment of the San Andreas Fault system. The aftershocks are scattered over a 30 km by 50 km area divided lengthwise by the nearly-parallel San Andreas, Zayante, and Sargent Faults. The polarisations of the leading split shear-waves are approximately fault-parallel (NW–SE) except at Station WAWA, some 7 km SW away from the Zayante Fault on the SW edge of the Basin, which are approximately NE–SW and parallel to the regional maximum direction of stress, σ_H. Zhang and Schwartz did not report temporal variations (which in any case are not expected and have not yet been observed during aftershock sequences [F14]).

Conclusions of Zhang and Schwartz [117] relevant to this review:

(1) The varying polarisations indicate anisotropy confined to the very shallow (uppermost 2 km) of the crust. There is a contrast between NE–SW at WAWA outside the fault zone and NW–SE within the fault zone.
(2) The lack of correlation of time-delays with depth and hypocentral distance also indicates shallow anisotropy above 2 km. Principally on the basis of these two conclusions, Zhang and Schwartz [117] infer that the cause of the fault-parallel polarisations is not wholly stress-aligned microcracks throughout the rock mass but also ''may result from mineral or fracture alignment caused by shearing along the plate boundary''.

Comments:

(1) The shallow crust would need to have such strong fracture-induced anisotropy to achieve the observed time-delays over short near-surface ray paths that the slower split shear-wave would be severely attenuated [F7]. The consistency of the many similar waveforms of the faster and slower split shear-waves illustrated by Zhang and Schwartz suggest this is not the case. If fluid-saturated cracks are the source of the anisotropy, as evidence in this review suggests, then the crack densities in the shallow crust suggested by Zhang and Schwartz would need to be so high that the crust would be close to disaggregation and the passage of any coherent shear-wave would be unlikely [F7]. The more consistent explanation is that the fault-parallel polarisations are 90°-flips caused by the high pore-fluid pressures near all seismogenic faults, which are observed at the surface only along major tectonic faults reaching nearly to the surface [43,44]. Station WAWA outside the fault zone has polarisations parallel to the regional stress field. This is exactly analogous to the pattern of polarisations at Parkfield [23] and at the Húsavík-Flatey Fault in Iceland [38]. The polarisations of shear-wave splitting at most stations of the Parkfield Network are parallel to the regional stress-field, whereas the polarisations at Station MM immediately above the San Andreas Fault, which at this point has a narrow fault zone, show 90°-flips and are fault-parallel and interpreted as the result of the critically-high-pressures on all seismogenic faults [44]. There is similar behaviour at the Húsavík-Flatey Fault [38].
(2) The ±80% scatter of time-delays and lack of correlation of time-delays with distance is typical of shear-wave splitting observed above all small earthquakes [5,6,45,46]. When the time-delays have such a large scatter, and a shear-wave velocity anisotropy that varies from positive to negative within the shear-wave window, any detailed correlation with distance or depth is likely to be hidden [F9, F10].

We suggest that the interpretations of Zhang and Schwartz [117] are subject to several fallacies particularly [F2, F7, F8, F9, F10]. The observed shear-wave splitting appears to be typical of that seen elsewhere, whose behaviour can be comprehensively interpreted as the result of compliant stress-aligned fluid-saturated microcracks throughout at least the upper half of the crust.

A.2.8. *Nadeau et al. [100] [F17]

*Nadeau et al. [100], as part of the Parkfield Earthquake Prediction Project, identified clusters of nearly identical earthquakes (doublets) for the years 1987–1992 within 5 km of a 25-km segment of the San Andreas Fault. They classified clusters by high cross-correlation coefficients in 63% of some 1700 earthquakes localised onto about 300 doublet-clusters of closely-spaced earthquakes. The analysis showed no progressive changes in waveform similarity amongst cluster members. The conclusion was that the structure around the cluster was stable.

Comments. The cross-correlation cluster analysis, as reported in [100], was principally aimed at identifying differences in *P*- and *S*-wave arrival times and was restricted to *vertical* component seismograms, including both *P*-wave and *S*-wave arrivals, where *S*–*P* time-delays were about 2 s. S-wave arrivals on vertical seismograms of local earthquakes are highly disturbed and cannot be used for reliable measurements [118]. Horizontal shear-wave seismograms within the shear-wave window are much more sensitive to small changes in stress, as a result of the critical nature of the distributions of stress-aligned fluid-saturated microcracks [7,38] but, as always, are subjected to the ±80% scatter in all observations of time-delays above small earthquakes [45]. Later (unpublished) discussions with Robert Nadeau confirmed that there were small, less than 0.1 s, changes between shear-wave arrivals on horizontal seismograms arrivals in each cluster which were too small to significantly affect the cross-correlation coefficients of the vertical components in the comparatively large time windows but are compatible with the time-delays reported elsewhere in this review [F17]. Thus, the seismograms analysed by *Nadeau et al. [100] are consistent with distributions of stress-aligned fluid-saturated microcracks showing temporal variations as suggested in this review. As far as we know, the horizontal seismograms of this data set have not been specifically examined for temporal changes in shear-wave splitting.

A.2.9. *Karageorgi et al. [101]

*Karageorgi et al. [101] analysed *P*- and *S*-wave recordings (1987–1995) at the 10-station Parkfield Earthquake Prediction Experiment network by repeated excitation of a shear-wave vibrator at up to six sites. Searching for evidence of temporal changes, they apparently did not specifically examine shear-wave splitting, but found several (20 to 30 ms) anomalies in *P*- and *S*-wave travel times that appear to be associated with earthquake source behaviour, such as variations in creep rate. They attribute these changes to variations in fluid content and are able to exclude near-surface water table changes. Although they do not mention cracks (or shear-wave splitting), the observations are generally compatible with changes due to the stress-sensitive fluid-saturated stress-aligned microcracks advocated in this review (also see Section A2.8, and *Nadeau et al. [99]).

A.2.10. Zinke and Zoback [119] [F2, F3, F4, F7, F8, F9, F10]

Zinke and Zoback [119] examined shear-wave splitting at Station HQR above small earthquakes before and after the 1986 Tres Piños earthquake in the South San Francisco Bay Area, California. The Tres Piños earthquake on the Quien Sabe Fault was 10 km east of the Calaveras Fault. Zinke and Zoback monitor splitting from two swarms. One small swarm (CP) is immediately beneath Cibo Peak ∼2 km west of the Calaveras Fault; and a larger swarm (QS) spanning the approximately parallel Quien Sabe fault system 10 km west of the Calaveras Fault. The polarisations of the CP swarm average NE–SW, approximately in the direction of the maximum horizontal compressional stress, σ_H, whereas polarisations at the QS swarm are approximately orthogonal and fault-parallel, averaging WNW-ESE.

Conclusions of Zinke and Zoback [119] *relevant to this review*.

(1) The upper layer of the crust (2–4 km) appears to be isotropic, as two different but stable polarisation directions are observed at the same station.
(2) The anisotropy around the Quien Sabe Fault appears to be controlled by the fault itself and probably caused by high pore-fluid pressures.
(3) In contrast, the anisotropy of the CP swarm, 4 km east of the Quien Sabe Fault system, appears to be controlled by the regional stress-field and is consistent with fluid-saturated microcracks.
    Comments:

(1) The two swarms, CP and QS, with different polarisations can be interpreted as the effects of uniform crack distributions on the 3D variations in directions of propagation. Polarisations from CP events, well within Band-1 directions to HQR [7], are parallel to the *maximum* horizontal stress direction σ_H, whereas polarisations from QS at the edge of the shear-wave window, on the edge of Band-1, are approximately parallel to the *minimum* horizontal stress, σ_h [7]. This is analogous to the 3D polarisations variations interpreted by *Gao and Crampin [24] (Section B2.5) and the 3D borehole observations of *Teanby et al. [37] (Section E2.3), where the effects of the 3D variations in polarisations were recognised. However, as always with shear-wave splitting, it is difficult to exclude alternative explanations, but

Table A1
Other observations of shear-wave splitting in California interpreted in terms of fluid-saturated stress-aligned microcracks

Reference	Source	Location and date	Possible temporal changes in shear-wave splitting time-delays.
Shih and Meyer [120]	Local earthquakes	South Moat of Long Valley Caldera (3 months, 1982).	Shih and Meyer [120] were not searching for temporal variations and time-delays are not plotted against time, but observations are generally consistent with stress-aligned fluid-saturated microcracks.
*Liu et al. [23]	Local earthquakes	Parkfield, San Andreas Fault (SAF) (1988–1990).	*Liu et al. [23] observed characteristic increases and precursory decreases before a M_L 4 earthquake comparable with those seen elsewhere, consistent with fluid-saturated stress-aligned microcracks.
Cochran et al. [121]	Local earthquakes recorded by six linear 800m arrays spanning the SAF.	Aftershocks of 1999, *M* 7.1, Hector Mine Earthquake during 1 year, 1999–2000).	Cochran et al. [121] did not observe temporal variations, but systematic changes are not expected in aftershock sequences [F14].

interpreting the observations as the expected azimuthal variations of a single widespread crack distribution, seems more likely than proposing the first known example of two differently polarised stress oriented anisotropic materials immediately next to each other. (Note that the other phenomena imposing orthogonal changes, 90°-flips associated with high pore-fluid pressures on seismogenic faults can probably be excluded. Such flips only occur within the immediate volume surrounding the fault, and paths from QS showing flips would need to pass immediately above the CP swarm which does not show flips.)

(2) Comment 1 suggests that the anisotropy around the Quien Sabe Fault is not fault controlled.
(3) Comment 1 also suggests that the anisotropy is almost certainly controlled by fluid-saturated microcracks.

A.2.11. Other observations of shear-wave splitting in California

Table A1 summarises three other studies of shear-wave splitting in California interpreted in terms of fluid-saturated stress-aligned microcracks, one of which showed temporal variations. *Liu et al. [23] observed characteristic (stress-accumulation) increases and (crack coalescent) decreases before a *M* 4 earthquake at Parkfield on the San Andreas Fault.

Appendix B. Temporal changes in shear-wave splitting before earthquakes in Iceland (Appendix B is summarised in Section 6.2)

B.1. Introduction

Iceland is above an offset of the Mid-Atlantic Ridge where, probably uniquely, two transform zones run onshore. Transform zones are highly seismic, and since there is an efficient seismic network and analysis system in Iceland [85], now accessible over the Internet, Iceland is a good place for studies of shear-wave splitting above earthquakes. Since 1996, there have been several EC-funded projects, PRENLAB 1 and 2, SMSITES, and PREPARED, during which shear-wave splitting has been continuously monitored. The monitoring still continues, but intermittently. Temporal variations in shear-wave time-delays monitoring stress-accumulation before earthquakes were recognised in Iceland by [5,46], and in 1988, the time, magnitude, and location of a *M* 5 earthquake in SW Iceland was successfully stress-forecast in a tight magnitude/time window [25].

As a result of some 10 years of monitoring in a region of persistent seismicity, much of our current understanding of shear-wave splitting above small earthquakes has come from analysis of shear-wave splitting recorded in Iceland. There are sufficient observations elsewhere to show that the Iceland results commonly apply worldwide (Appendices A, C, D and E). These studies pioneered the current understanding of shear-wave splitting as the result of propagation through distributions of stress-aligned fluid-saturated microcracks so closely-spaced that they are critical-systems verging on fracture-criticality, fracturing, and earthquakes [10,11,41,42]. Many aspects of this study are summarised in Table 2 of the main text, and will not be repeated here. Only the more significant items are listed below.

B.2. Observations of shear-wave splitting

B.2.1. Menke et al. [55] [R1]

Menke et al. [55] were probably the first to report shear-wave splitting in SW Iceland. The splitting was attributed to vertical stress-aligned cracks. The results and conclusions are generally compatible with the observations of *Volti and Crampin [5,46] and others in SW Iceland suggesting the cause is stress-aligned *microcracks*. The possibility of temporal variations was not examined.

B.2.2. *Crampin et al. [25] [R1, R2, R3, R6]

The first successful stress-forecast earthquake. In October 1998, *Crampin et al. [25] recognised during the 4-year study reported in Section B2.3, below, that shear-wave time-delays were increasing in Band-1 directions at stations BJA and SAU in SW Iceland. The rate of increase was similar to that before a *M* 5.1 earthquake some 6 months earlier near BJA [5]. Based on the estimated duration of the increase and approach to levels of fracture-criticality, an email alert was sent to the Iceland Meteorological Office (IMO) on 10th November, 1998, stating that "*…an event could any time between now (M ≥ 5) and end of February (M ≥ 6)*." Following an earlier email on 27th October, 1998, Ragnar Stefánsson (IMO) had suggested that the increase might be linked to the continuing seismic activity associated with the previous *M* 5.1 earthquake. Three days later, on 13th November IMO reported "*…there was a magnitude 5 earthquake just near to BJA (preliminary epicentre 2 km west of BJA) this morning 10 38 GMT*", fulfilling the forecast in a narrow time/magnitude window [25]. We suggest that this is the first scientifically, as opposed to precursory or statistically, predicted earthquake, and provides direct proof that variations of shear-wave splitting can forecast earthquakes. Logarithms of the duration of the increases are approximately proportional (self-similar) to the magnitudes of the eventual earthquakes.

Note that Seher and Main [60] commented adversely on the statistics underlying the forecast. *Crampin et al. [61], in response, demonstrated that the criticisms of Seher and Main were invalid for analysing isolated increases superimposed on a continuous time series (see Item 5, Table 3).

Note that the successful stress-forecast [25] has not been repeated because the severe restrictions on appropriate source–geophone-earthquake geometry are difficult to meet. (The appropriate geometry requires sufficient shear-wave ray paths in Band-1 directions with in the shear-wave window.) The only other suitable earthquake was not stress-forecast because of seismic quiescence at a critical time so that there were insufficient shear-wave source events and the stress-accumulation was not recognised [30] (see discussion in Section B2.6, below).

B.2.3. *Volti and Crampin [5,46] [R1, R2, R3, R6]

Volti and Crampin [5,46] reported a 4-year study of shear-wave splitting in Iceland. This study and its associated papers established much of the current understanding of shear-wave splitting. Changes of shear-wave time-delays were observed before five earthquakes (the last of which was the successfully stress-forecast earthquake, see previous section). These five earthquakes occurred during a 2-year approximately linear decrease in normalised time-delays of ∼2 ms/km/year following the 1996, Gjàlp eruption, on the Vatnajökull Ice Cap, during which extraneous magma-induced disturbances were minimal (Section D2.1). Since that time, minor magmatic activity has considerably disturbed the typical self-similar behaviour of time-delays before earthquakes and no further earthquakes have been stress-forecast in real-time, but see Section B2.6, below.

B.2.4. *Gao and Crampin [6] [R1, R3, R6]

Gao and Crampin [6] recognised that, at the ends of the *increases* of time-delays in Band-1 directions interpreted as monitoring stress-accumulation before larger earthquakes, there are also *decreases* in time-delays immediately before impending earthquakes. These occur in all cases where there were sufficient source data before the event. Such a decrease was first recognised in the Enola Swarm, Arkansas by *Booth et al. [22]. *Gao and Crampin initially interpreted these decreases as some form of (unspecified) stress relaxation. However, it is now recognised [24,30,44,45] that the decrease is the result of coalescence of microcracks into larger cracks as the eventual fault-plane is identified during the stress-accumulation. Fig. 6 is a key figure from [6] showing the consistency of the increases and decreases of time-delays before larger earthquakes. The logarithms of the durations of both stress-accumulation increases and crack coalescence decreases are self-sim-

ilar and separately proportional to the earthquake magnitudes (Fig. 7). Note that this paper [6] is included in this Appendix on Iceland as three of the six earthquakes are in Iceland.

B.2.5. *Gao and Crampin [24] [R1, R2, R3, R5, R6]

*Gao and Crampin [24] showed that spatial changes in the location of shear-wave source earthquakes, showing temporal variations before a M 4.9 earthquake in N Iceland, could cause anomalies in shear-wave polarisations, which are not caused by high-pressure-generated 90°-flips. For thin parallel stress-aligned fluid-saturated microcracks the polarisations of the faster split shear-waves are parallel to the direction of maximum horizontal stress in a $\pm\sim30°$-wide band across the centre of the shear-wave window [7]. Outside this band, but still within the shear-wave window, the polarisations are approximately orthogonal to the stress direction. Gao and Crampin show that the spatial variations in locations of the source earthquakes are compatible with this interpretation. Zinke and Zoback [119] (see our re-interpretation, Section A2.10) and *Teanby et al. [37] (Section E2.3) display similar ray path-dependent variations in polarisation.

B.2.6. *Wu et al. [30] [R1, R2, R3, R5, R6]

*Wu et al. [30] re-examined shear-wave splitting before a pair (4 days apart) of $Ms \sim6.6$ earthquakes in June 2001 in SW Iceland. These were the largest earthquakes in Iceland for several decades and had not been stress-forecast by variations in shear-wave splitting. This was because there was a 2-month quiescence of the source events at the beginning of the (now identified) 6-month stress-accumulation. Without shear-wave source earthquakes the increase was not recognised. *Wu et al. [30] showed that quiescence before this earthquake was extensive over most of Iceland. In order to examine this earthquake in more detail the Iceland Meteorological Office extended the seismic catalogue (and Internet seismograms) to include earthquakes down to magnitude M 0 and below. Using this extended data set, *Wu et al. [30] showed that the $Ms \sim6.6$ earthquakes displayed the characteristic stress-accumulation increase and the crack coalescence decrease typical of earthquakes worldwide. *Wu et al. also showed that durations of both the increase and decrease were (separately) self-similar with those of the other Iceland earthquakes (Fig. 7).

Appendix C. Temporal changes in shear-wave splitting before earthquakes elsewhere (Appendix C is summarised in Section 6.3)

C.1. Introduction

Apart from California (Appendix A) and Iceland (Appendix B), and to a lesser extent Italy (C2.4) and New Zealand (C2.7 and C2.8), below, the Band-1 constraints on observing temporal changes, studies of shear-wave splitting elsewhere are met only for chance coincidence of swarms of earthquakes, seismic stations within the shear-wave window, and suitable larger earthquakes nearby. These larger earthquakes were sometimes within the swarm sequence itself and sometimes nearby.

C.2. Observations of shear-wave splitting

C.2.1. Arkansas, USA: *Booth et al. [22] [R1, R2, R3]

The first observation of precursory (crack coalescence) decreases: *Booth et al. [22] observed shear-wave splitting at a temporary network operating for 12 days above a swarm of small earthquakes near Enola, Arkansas. *Booth et al. identified an increase in time-delays in Band-1 of the shear-wave window, on a sparse data set, 4 days before a magnitude M_L 3.8 swarm earthquake interpreted as monitoring stress-accumulation. *Booth et al. [22] also identified a precursory decrease starting 12 h before the earthquake. This was the first time a decrease indicating some form of precursory stress relaxation had been recognised. (The precursory decrease before the North Palm Springs Earthquake, *Peacock et al. [27], was not recognised until *Gao and Crampin [6] identified precursory decreases before five other earthquakes, see Section B2.4, above.) These decreases are now interpreted as the effects of crack coalescence as micro- and macro-cracks converge on the impending fault break. Such decreases have now been identified before some nine earthquakes worldwide (Table 1b). The logarithms of the durations of both increases representing stress-accumulation, and decreases

representing precursory crack coalescence, are self-similar and approximately proportional to the earthquake magnitudes (Fig. 7).

C.2.2. China: *Gao et al. [21]; *Gao et al. [6,26] [R1, R2, R3]

There have been two observations of temporal changes in shear-wave splitting before earthquakes in China. *Gao et al. [21] observed temporal changes before a magnitude M_L 3.6 earthquake above a swarm of small earthquakes near Dongfang, Hainan Island, China, but the data are sparse. The logarithm of the duration of the stress- accumulation increase has a similar self-similar relationship with magnitude as those observed elsewhere. The data were too sparse to indicate a consistent decrease. *Gao et al. [6,26], in another sparse data set, observed temporal increase in time-delays before a M_S 5.9 earthquake in Shidan, Yunnan, China and a precursory decrease before a M_S 5.3 earthquake nearby. Both increase and decrease have similar self-similarity relationships with magnitude to those seen elsewhere. In both cases, observations and interpretations are consistent with the fluid-saturated microcracks reported in this review.

C.2.3. Hawaii: Munson et al. [122] [F2, F5, F6, F7, F8, F9, F10]

Munson et al. [122] examined shear-wave splitting recorded at a permanent Station AIN before and after the 1983 M_L 6.6 Kaoiki Earthquake in Southern Hawaii and also later at four temporary arrays. The temporary arrays were deployed within 30 km of the earthquake epicentre for several months in 1990, some 7 years after the Kaoiki Earthquake.

Conclusions of Munson et al. [122] relevant to this review.

(1) The observed shear-wave polarisations are generally consistent with information on stress orientation and indicate crack-induced anisotropy. However, although the polarisations are generally consistent within each array, there are ''sharp'' variations in polarisations at different arrays, which [122] interpret as indicating shallow anisotropy.
(2) A weak correlation of time-delays with epicentral distance and focal depth also suggest shallow anisotropy with shear-wave velocity anisotropy exceeding 10%. This indicates a highly fractured upper crust suggesting the possibility of strong near-surface structural anisotropy.
(3) There was no evidence reported for temporal variations in delay-times before and after the main shock.

Comments:

(1) Shear-wave polarisations are extremely sensitive to surface topography. The free-surface beneath the temporary arrays on Hawaii has highly irregular topography, as demonstrated by ''gulch'' in the names of two of the four arrays, and the polarisations necessarily display topography-induced scatter. Shear-wave polarisations, and the effective shear-wave window, are highly dependent on the incidence angle to the free-surface. The overall topographic slope of ∼1/8 (∼7°) at the arrays on the side of the volcano, as well as the local irregularities, will modify the edge of the effective shear-wave window and disturb polarisations. The overall directions of polarisation of three of the arrays point are approximately up-slope towards Mauna Loa, the highest volcano in Southern Hawaii. This suggests: that either polarisations are controlled by the topographic slope rather than the subsurface anisotropy [F6]; or that maximal horizontal stress radiates from the summit; or most likely a combination of both phenomena. The exception is Bird Park Array, which is within 5 km of the large caldera of the highly active Kilauea volcano, where local movement of magma is expected to modify the stress-field, modify microcrack orientations, and hence modify shear-wave polarisations. These various anomalies suggest that polarisations are dominated by topographic irregularities rather than stress orientations.
(2) The known ±80% scatter in time-delays, typically observed above small earthquakes due to 90°-flips in shear-wave polarisations [45], is so large that correlation of time-delays with epicentral distances or focal depths are typically weak or hidden as in Hawaii [F10]. Consequently, strong shallow anisotropy cannot necessarily be inferred.

(3) Observations of temporal variations in time-delays require stringent source-to-recorder geometry. Only time-delays in Band-1 directions of the shear-wave window are sensitive to the low-level changes of stress accumulation before earthquakes [7]. Time-delays were recorded at Station AIN for 230 days before and 10 days after the main shock. Band-1 and Band-2 data points are not identified, but the equal-area polar projections indicate that there are very few, perhaps 6–10 data points (5–10% of the total), with Band-1 directions, and temporal variations in time-delays would not be expected in substantially Band-2 directions which do not typically display temporal variations for low-level changes of stress [7].

We suggest that the interpretations of Munson et al. [122] are subject to several fallacies particularly [F2, F5, F6, F7, F8, F9, F10] in Table 4. Again the shear-wave splitting observed by Munson et al. appears to be typical of that seen elsewhere, whose behaviour can be comprehensively interpreted as the result of compliant stress-aligned fluid-saturated microcracks.

C.2.4. Italy: *Del Pezzo et al. [104] [R1, R2, R3, R6]

*Del Pezzo et al. [104] monitored shear-wave splitting at a network of seismic stations above a swarm of small earthquakes 2–4 km lower than the summit crater of Mt. Vesuvius. Both the surface and internal topographies are irregular. The two stations, BKN and BKE, nearest to the summit are on an approximately horizontal surface within the larger ancient caldera (Mt. Somma) and earthquakes within the shear-wave window display fast split shear-wave polarisations approximately in line with the summit cone suggesting maximum stress radiating from the central volcano pile. Time-delays, normalised to s/km, in Band-1 directions at the nearest station, BKN, 1 km to the north of the summit crater, display a ∼86-day increase (our interpretation) and precursory ∼10-day decrease, before a larger magnitude M_L 3.6 earthquake (October 1999), which was the largest earthquake within the Vesuvius region since 1944. *Del Pezzo et al. [104] recognise that the shear-wave splitting is monitoring crack deformation.

The Band-1 time-delays at the next-nearest station, BKE, 1.5 km to the east of the summit, are much more scattered. They show an irregular less-pronounced increase, no precursory decrease, and another more minor increase ∼30 days after the 3.6 earthquake.

Note that *Del Pezzo et al. [104] also report temporal changes in the b-value of the Gutenberg–Richter relationship and the coda decay rate for this M_L 3.6 earthquake.

Comments. The increase in Band-1 time-delays at BKN, interpreted as stress-accumulation, and the decrease, interpreted as crack coalescence, are typical of those observed elsewhere as reported throughout this review and are compatible with shear-wave splitting monitoring fluid-saturated microcrack geometry. However, the values of the normalised time-delays of up to ∼40 ms/km are much larger than are usually observed elsewhere. Larger values, up to ∼20 ms/km are found in Iceland, where they are attributed the effects of the generally high heat-flow [5,46]. The size of time-delays depends on many parameters including: Poisson's ratio; P- and S-wave velocities of the rock matrix; and temperature [83]. High heat-flow is believed to be the cause of high values on Vesuvius. The reason for the exceptionally large duration of ∼86 days before a small M_L 3.6 earthquake again is not understood. It is probably related to the exceptional stability of Vesuvius, which has minimal seismic and volcanic activity. The durations of the increases in time-delays are thought to be related to the rate of stress/strain increase in the surrounding area, and there is no known reason why the rates should be similar for earthquakes and volcanoes in different regions.

Note that only 18-point moving averages of time-delays are plotted. This leads to simplification of variations with time, but hides the ±80% scatter which appears to be a diagnostic and characteristic feature of time-delays above all small earthquakes [10,45]. 18-point moving averages could also hide significant variations, such as the duration of increasing stress, if the variations are only represented by a few data points. This can be compared to plotting a least-squares line without plotting the data points: valuable inferences may be hidden.

Note also that the plots of temporal changes of time-delays before the M_L 3.6 earthquake on Vesuvius of *Del Pezzo et al. [104] are almost identical to the variations seen before a flank eruption at Mt. Etna, Sicily by *Bianco et al. [32], discussed in Section D2.3 of Appendix D.

C.2.5. Japan: Kaneshima [123] [R1, R3]; Volti et al. [124]; *Saiga et al. [105]; *Hiramatsu et al. [125]

Kaneshima [123], in 1990, in an early review of extensive observations of shear-wave splitting reported shear-wave splitting in Honshu and Shikoku, Japan. Kaneshima did not seek nor report evidence of temporal changes. Volti et al. [124] identified sea-mounts in the Nankai Trough by their effect on shear-wave polarisations but did not seek temporal changes. Two papers studied temporal changes associated with the 1997, M_W 5.7, Aichi-ken Tobu earthquake beneath the Tokai region of Honshu, Japan [105,125].

*Saiga et al. [105] monitored shear-wave splitting above small earthquakes for ∼11 years before and ∼2 years after Aichi-ken Tobu earthquake. The shear-wave polarisations are consistent with the regional stress-field from earthquake fault-plane mechanisms. *Saiga et al. did not report temporal changes before the earthquake but identified increases in time-delays (in seconds) at the time of the M_W 5.7 earthquake in both Band-1 and Band-2 directions for source earthquakes in both the crust (depth <25 km) and the subducting slab (depth ⩾25 km). A neighbouring station INU showed shear-wave splitting but did not show temporal variations at the time of the earthquake. Both stations showed the typical ±80% scatter about the mean. The level of shear-wave velocity anisotropy at 0.6% was very low, and *Saiga et al. concluded that the Aichi-ken Tobu earthquake was too deep at 39 km and the velocity anisotropy too small to show precursory changes in time-delays as identified in [27–29].

*Hiramatsu et al. [125], continuing the analysis of *Saiga et al., studied the increase of (normalised) time-delays following the Aichi-ken Tobu earthquake. The time-delays for both crustal and slab source earthquakes peaked in value and in both cases decreased to the ambient level over about 18 months. Hiramatsu et al. interpreted this as indicating crack healing similar to that reported in laboratory experiments.

Comments: *Saiga et al. [105] did not report changes in time-delays before the Aichi-ken Tobu earthquake, however, Fig. 7 of that paper shows five-point moving averages of time-delays (in seconds) at STN before the event where both crustal and slab source events show increases from the average ambient level. For both crustal and slab sources, the time-delays approximately double in value over about 18 months before the event. Thus the time-delays show similar stress-accumulation increases with rates of increase as those observed elsewhere. The data is sparse and it is difficult to access the exact duration of the increase. Crack coalescent decreases are not visible.

*Hiramatsu et al. [125] did not separate Band-1 and Band-2 directions, and this is the first time that peaks of time-delays have been identified *after* earthquake. It may be the shear-wave splitting behaves differently in subducting slabs. The combined directions do not show the stress-accumulation increase of *Saiga et al. [105].

C.2.6. Kamchatka: Krasnova and Chesnokov [126]; Luneva and Lee [127] [R1, F6]

Krasnova and Chesnokov [126] monitor shear-wave splitting at ten stations near Petropavlovsk, Kamchatka, for shear-wave arrivals from 35- to 55-km deep earthquakes up to 100 km offshore in the Gulf of Avacha. One station, PET, shows orthogonal changes in rose-diagrams of shear-wave polarisations before and after an offshore M 4.5 earthquake. Other stations show minor variations in shear-wave polarisations, but not orthogonal changes. Krasnova and Chesnokov [126] suggest these changes are temporal variations in shear-wave splitting.

Comments. Many of the earthquakes are outside the straight-line shear-wave window (see Item 2, Section 2.2) for some or all of the stations. For shear-wave propagation in distributions of thin vertical cracks, the faster split shear-wave is theoretically polarised *parallel* to the direction of maximum horizontal stress in a typically ±40°-wide band across the centre of a polar projection [7] (allowing for refraction through low-velocity layers). This was observed by *Teanby et al. [37], *Gao and Crampin [24], and in our interpretation of Zinke and Zoback [119]. For arrivals outside this band, the shear-wave polarisations are approximately *perpendicular* to the polarisations within the band. Epicentres of the earthquakes in the [126] data set have different distributions before and after the M 4.5 event, and the changes in polarisation are almost certainly caused by spatial rather than temporal variations, as demonstrated by *Gao and Crampin [24]. If the [126] data set does show temporal changes, it is the only occasion that changes in polarisations have been observed to occur during earthquake preparation (as opposed to 90°-flips before volcanic eruptions [32,33]), and this seems unlikely. All other examples of temporal changes before earthquakes only show changes in time-delays.

Luneva and Lee [127] also monitor shear-wave splitting at Station PET using shear-waves from 40- to 184-km deep earthquakes off-shore at less than 100 km from PET and are within the shear-wave window. They

divide their shear-wave source earthquakes into two sets above and below 80-km depth. The normalised time-delay points are sparse: 19 earthquakes above and 32 below 80 km, set in our Band-1 (their Band-2) directions in 3 years. Their three-point moving averages of statistical interpolation show variations with time that are interpreted as indicating temporal changes in shear-wave splitting.

Comments. The association of variations with large earthquakes is weak and suspect, because the data are sparse and the ±80% scatter always observed above earthquakes [45] is ignored. Hence temporal variations in shear-wave splitting in Kamchatka are unproven in both [126] and [127] data sets.

C.2.7. New Zealand I [R1, F2, F7, F8, F9, F10]

Shear-wave splitting in the Wellington Peninsula. There have been several studies of shear-wave splitting in the crust in New Zealand (*Gledhill [54,102,128], Audoine et al. [129,130], amongst others), but temporal variations were not identified and were specifically denied. *Gledhill [54] records nearly-parallel shear-wave polarisations above 15- to 60-km deep earthquakes at a temporary deployment of seismic stations on the topographically-irregular Wellington Peninsula, New Zealand. The Wellington Peninsula has irregular topography varying in height from sea level to 500 m.

Gledhill [54] conclusions relevant to this review:

(1) Large station-to-station changes in polarisations are observed, even for stations as close as 3.5 km, which is interpreted as indicating anisotropy confined to the uppermost few km of the crust.
(2) Similar polarisations (and time-delays) are seen for direct arrivals from an earthquake at 34.8-km depth as for *P*-to-*S* conversions at the plate boundary implying consistent shear-wave anisotropy throughout the crust.
(3) Gledhill finds no evidence for temporal changes.

Comments:

(1) The variations in polarisations are almost certainly due to the highly irregular surface topography around each station disturbing the effective shear-wave window [118].
(2) The observed consistency of splitting throughout the crust is an important indication of the depth-range of crack-induced shear-wave splitting. See discussion in Section 7.2 of the main text.
(3) *Gledhill [54] plots the variation of time-delays with time duration at four stations but does not identify temporal variations in the typical ±80% scatter. However, the plots at three of the stations show initially high values of time-delays within the first 45 days of the deployment, a drop in values, and all four stations show an average increase from day 45 for the whole of the remaining ∼160 days duration of the network. *Gledhill [102] continuing the study of shear-wave splitting in the Wellington Peninsula lists large earthquakes nearby. The two largest events associated with the recording period of the *Gledhill [54] deployment were a *M* 5.1, 151-km deep, earthquake at 157 km epicentral distance immediately after the drop in time-delays at about day 45 in the plots of *Gledhill [54], and a *M* 6, 122-km deep, earthquake at 135 km distance some 30 days after the end of the recording period at day 164. Thus it is possible that the increase in time-delays monitors the stress-accumulation before the *M* 6 earthquake. Certainly, evidence elsewhere suggests that a *M* 6 earthquake would be expected to modify shear-wave splitting at such distances [5,24,46], and the 115 days duration of the increase is compatible with the self-similarity seen elsewhere [24,30]. Plots at three of the stations also show evidence for precursory decreases monitoring crack coalescence before the *M* 5.1 event. Thus it appears that *Gledhill [54] presents plots showing examples of temporal variations in shear-wave splitting before earthquakes compatible with those observed elsewhere.

Note that the plots in *Gledhill [54] cannot be interpreted directly as the plot includes arrivals within the whole of the shear-wave window. Most of the data points appear to be in Band-2 directions which are typically not sensitive to small changes of stress, and only a small proportion of the data points are Band-1 directions, which are sensitive to stress-accumulation [7].

Note also that shear-wave polarisations at the three stations showing temporal variations are approximately WSW-ENE close to the orientation of the pervasive faults, SW-NE, throughout the Peninsula, whereas polarisations at the other station are approximately orthogonal at NNW-SSE in the direction of the ambient regional stress-field. These temporal variations in time-delays for both fault-parallel and stress-parallel polarisations confirm that the shear-wave splitting is caused by microcracks, as at KNW, California [27], despite the reasons for the changes in polarisations not being wholly understood.

C.2.8. New Zealand II [R1, F1, F2, F7, F8, F9, F10]

Shear-wave splitting in the Marlborough Region. Balfour et al. [103] is a comprehensive study of stress and shear-wave splitting in the Marlborough Region of South Island, New Zealand, some ~50 km across the Cook Straight from the Wellington Peninsula, North Island [54]. Balfour et al. make very consistent stress-inversions of fault-plane mechanism, which lead to a WNW-ESE maximum horizontal stress making an angle of about 60° to the dominant WSE-ENE faulting throughout the Marlborough Region. They analyse shear-wave splitting for earthquakes less than 25 km in depth. There is a wide scatter in shear-wave polarisations but the average polarisation is approximately fault-parallel at about 60° to the stress direction. Balfour et al. do not search for temporal variations in time-delays.

Conclusions of Balfour et al. [103] relevant to this review:

(1) Since the stress is ~60° to the average fault strike, they conclude that the faults are weak due to a low coefficient of friction or a high pore-fluid pressure.
(2) The spatial variations in shear-wave polarisations suggest that the anisotropy is in the uppermost 15 km of the crust.
(3) The shear-wave polarisations are ~60° to the stress-field and are thought to be not induced by crack geometry but "related predominately to the geological structure and not to the ambient stress-field" (and crack geometry).

Comments:

(1) Weak faults due to high pore-fluid pressures agrees with the interpretation and modelling of shear-wave splitting time-delays by Crampin et al. [44,45] and many other studies throughout this review.
(2) The Marlborough Region is highly irregular topographically with mountains over 2000 m and many slopes of 10° to 20°. The sensitivity of shear-wave polarisations to irregular topography is almost certainly the cause of the observed scatter. A large scatter, in particularly of shear-wave polarisations, is one of the inescapable penalties of recording shear-wave splitting in mountainous areas [5,45,46,118].
(3) The geological structure-parallel polarisations and stress-parallel polarisations in the Marlborough Region are broadly similar to the polarisations in the neighbouring Wellington Peninsula of *Gledhill [54], see previous section, which we suggest shows evidence of temporal changes in time-delays that are necessarily caused by crack anisotropy. The shear-wave polarisations in the shear-wave window directly imply TIH-anisotropy, or a minor variation thereof, and strongly suggests stress-aligned microcracks. Other anisotropic symmetries may lead to very different polarisations. Polarisations in the Marlborough Region are generally restricted to parallel rose-diagrams which are strongly diagnostic of distributions of parallel vertical cracks [R1]. (The principal exceptions are Stations GOHM2 and ALIE5 which display a wide range of polarisations, typical of stations sited near mountainous peaks where scatter in polarisations is expected due to the interaction of shear-waves with surface topography [5,24].)

Note the nearly-parallel polarisations and corresponding nearly-parallel rose-diagrams for ray paths over the whole range of the shear-wave window. It is highly unlikely that geological configurations other than stress-aligned microcracks could lead to the observed polarisations.

Appendix D. Temporal changes in shear-wave before volcanic eruptions (Appendix D is summarised in Section 6.4.)

D.1. Introduction

Changes in Band-1 time-delays are believed to monitor low-level changes of stress [7,43]. Such stress changes are expected to occur before earthquakes (Appendices A, B, C), but also before other changes of stress during other tectonic activity such as preparations for volcanic eruptions. This appendix presents evidence for temporal changes in shear-wave splitting before eruptions at three volcanoes: a major eruption of Gjàlp. beneath the Vatnajökull Icefield, Iceland; and more minor volcanic episodes on Mt. Ruapehu, New Zealand, and Mt. Etna, Sicily.

D.2. Temporal changes before volcanic eruptions

D.2.1. Iceland [R1, R2, R3, R6]
*Volti and Crampin [5] observed temporal increases in Band-1 time-delays for 5 months at ∼240-km distance in directions N, SW, and WSW before the 1996 Gjàlp Eruption on the Vatnajökull Icefield, which was the largest eruption in Iceland for several decades. The eruption opened a 10 km, approximately NS fissure. The increasing time-delays were interpreted as indicating the accumulation of stress as the ascending magma *magma fractures* the upper crustal surface layers (presumed to be equivalent to hydraulic fracturing in the oil industry).

The pattern of increase in time-delays was typical of the increases now seen before many earthquakes in Iceland and elsewhere, except that time-delays before earthquakes characteristically decrease immediately stress is released at the time of the earthquake or (when data is available) in a crack coalescence stress relaxation immediately before the earthquake. However, the increase in normalised time-delays at Gjàlp does not decrease at the time of the eruption but gradually declines at about 2 ms/km/year over the following 2 years visible in both Band-1 and Band-2 directions at four widely separated Stations BJA, GRI, KRI, and SAU in Iceland. The expanded magma-filled fracture (dyke) is a permanent feature and the 2-year decrease in time-delays following the eruption is interpreted as the Mid-Atlantic Ridge adjusting to the movement of Iceland imposed by the massive dyke injection.

Iceland is highly active tectonically. Following Gjàlp, there have been several changes of time-delays which appear to be associated with minor volcanic episodes but are difficult to evaluate, particularly as the magnitude of magmatic activity is difficult to assess and quantify. This magmatic activity also makes it more difficult to interpret the increases before earthquakes. The 2-year decrease in time-delays was approximately linear, and there appeared to be no other significant magmatic disturbances during this time, which was the interval when changes before five earthquakes, some small, were recognised (Table 1) [5,25].

D.2.2. New Zealand [R1, R2, R3, R5, R6] [F2, F5, F12]
*Miller and Savage [33] report orthogonal changes in shear-wave polarisations during an eruption of Mt. Ruapehu, New Zealand, where the shear-waves are from earthquakes deeper than 50 km. Their conclusions are that increased magmatic pressure in injected vertical dykes, striking parallel to the regional stress direction, caused 90°-flips in shear-wave polarisations which are reversed, when the eruption releases some of the pressure. Such shear-wave polarisations orthogonal to regional stress are claimed to be a possible indicator of impulsive andesite eruptions, which are otherwise difficult to predict.

Comments. These changes in polarisation appear to be the magmatic equivalent of the 90°-flips observed and modelled when there are critically-high hydraulic pressures [35,44,45]. In a later paper, *Gerst and Savage [47] prefer to argue for magmatic pressure-induced reorientation of large fractures as the cause of the orthogonal changes in shear-wave polarisations, rather than the microcrack 90°-flip model. Since effective shear-wave splitting requires wavelengths greater than crack dimensions, distributions of large fractures are unlikely to yield effective shear-wave splitting from high-frequency crustal

earthquakes. Fixed orientations, inducing sufficient 90° changes in orientation to alter shear-wave polarisations also seems unlikely.

Note that the changes in polarisation in the 90°-flip model of Crampin and Zatsepin [42] are the result of fluid pressures modifying the directions of maximum horizontal stress in a (usually) small volume surrounding the source of the pressure by critically-high-pressure fluids on the impending fault. This suggests that the volume will also display fault-plane mechanisms with anomalous stress directions as well as 90°-flips in shear-wave splitting. Such 90°-flips as crack reorientations above 50-km deep earthquakes as observed beneath Mt. Ruapehu also supports the suggestion of Crampin [111] that shear-wave splitting in the upper-mantle is, at least partially, caused by crack-induced anisotropy, where the cracks are films of hydrated melt around partially melted grains.

D.2.3. Italy [R1, R2, R3, R5, R6]

*Bianco et al. [32] monitored shear-wave splitting recorded by two stations of a permanent seismic network, above a swarm of earthquakes on Mt. Etna, Sicily, before and after a flank fissure eruption. One station, MNT was very close to the fissure and was damaged by the erupted lava. The other station, ESP, was further from the fissure but still within Band-1 directions in the shear-wave window above an earthquake swarm below the fissure. Note that, as with *Del Pezzo et al. [104], only 18-point moving averages of time-delays are plotted, which lead to simplified more-easily interpretable variations but hide the characteristic ±80% scatter in time-delays.

There are changes in time-delays at MNT and ESP, and changes in shear-wave polarisations at MNT. The plot of time-delays shows the typical characteristic behaviour: a long-term increase at both stations starting "at least 20 days before the eruption" and a decrease "starting 2–3 days before" the eruption. These are similar to those observed before earthquakes elsewhere [5,6]. (Our preferred interpretation of the plots suggests that the increase starts ∼66 days before the eruption and the decrease some 5 days before, however the 18-point moving average tends to hide these details.)

The polarisations of the faster split shear-wave at ESP showed little variation. However, the polarisations at MNT show several abrupt 90° changes interpreted as the effects of 90°-flips in crack orientations caused by high fluid pressure, as in the critically-high pore-fluid pressures on all seismically-active faults [42–44]. The most persistent 90°-flip starts ∼66 days before the eruption when the time-delays begin to increase, and reverses (to the initial polarisation oriented towards the volcanic cone) at the time of the eruption, just before MNT was damaged by the eruption.

Comments. 90°-flips can be interpreted as reorientations of fluid-saturated microcracks in the immediate vicinity of the dyke injection as the pressures approach levels inducing fracture-criticality when the magma fractures the surface layers as the eruption begins. This is similar to the 90°-flips seen before the eruption of Mt. Ruapehu by *Miller and Savage [33], see previous section. The flips are also seen above major faults cutting the crust [40] and can be modelled as the cause of the ±80% scatter in time-delays observed above all seismically-active faults [45].

These observations are compatible with the anisotropy-induced by stress-aligned fluid-saturated microcracks. One interesting feature of these observations, is that the variation of time-delays with time before the eruption is almost identical with variations before the *M* 3.6 earthquake in the swarm of earthquakes on Mt. Vesuvius (BKN in Fig. 9 of *Del Pezzo et al. [104], see Section C2.4). This suggests two phenomena: (1) shear-wave splitting monitors the effects of stress on the fluid-saturated microcracks in almost all rocks independent of the source of the stress change; and (2) the strong similarity of both the accumulation of stress and the suggested crack coalescence suggests that the stress regimes in the source zones of earthquakes and, at least some, volcanic eruptions are similar. However, a major difference is that following an earthquake, time-delays (and inferred crack geometries) abruptly return to the background values as stress is released by fault slip, whereas following eruptions time-delays do not immediately return to background levels, but relax more slowly as the crust responds to the injected magma. Following this eruption, the time-delays at ESP on Mt. Etna [32] returned to the background level in a two-stage process over ∼50 days. Following the much larger Gjàlp Eruption in Iceland, the return to the background level took 2 years [5] (Section D2.1, above).

Appendix E. Other observations of temporal variations in shear-wave splitting (Appendix E is summarised in Section 6.5.)

E.1. Introduction

   When small earthquakes are used as a source of shear-waves, the source is poorly understood and uncontrollable. Consequently, controlled source experiments are valuable for monitoring changes in shear-wave splitting, and are also free of the anomalous ±80% scatter in time-delays caused by 90°-flips in shear-wave polarisations as a result of the critically-high pore-fluid pressures on seismically-active faults [44,45]. If experiments are sufficiently below the surface in bore holes, the observations are also free of the constraints imposed by the shear-wave window at a free-surface, although they may be disturbed by the usually more minor effects of the internal shear-wave windows at each interface [82].

E.2. Observations of shear-wave splitting

E.2.1. Fluid-injection I: *Angerer et al. [35] [R1, R2, R4, R5]
   *Angerer et al. [35] used APE to model the time-lapse response of a fractured carbonate reservoir to both high-pressure and low-pressure CO_2-injections as imaged by reflection surveys of an areal array of a 25-m grid of three-component geophones recording a similar grid of shear-wave vibrators. The dominant seismic effects were on the arrival times and time-delays of the split shear-waves [34]. *Angerer et al. [45] selected an initial model with a distribution of cracks to match the initial observations of shear-wave splitting with synthetic seismograms calculated by ANISEIS [131,132], a commercially-available programme for calculating full-wave synthetic seismograms propagating through a plane-layered multi-layered anisotropic halfspace. *Angerer et al. [35] then inserted the exact values of the injected pressures into APE, recalculated the modified reservoir structure, and recalculated the synthetic seismograms with the modified parameters, obtaining an almost exact match of observed to calculated shear-wave splitting for both high- and low-pressure injections. This shows that APE appears to be a satisfactory model of cracked fluid-rock deformation, and *Angerer et al. [35] is the best *in situ* calibration of APE-modelling to-date.

E.2.2. Fluid-injection II: *Bokelmann and Harjes [36] [R1, R2, R3, F9, F12] [F9, F12]
   *Bokelmann and Harjes [36] report the effects on shear waves of fluid injection at 9-km depth in the KTB deep drilling site [133] in SE Germany. *Bokelmann and Harjes observed shear-wave splitting from injection-induced events at a borehole recorder at 4000-m depth in a pilot well offset 190 m from the KTB well.
   Conclusions of *Bokelmann and Harjes [36] relevant to this review:

   (1) There are temporal variations in shear-wave splitting from injection-induced events. In particular, the initial ~1% shear-wave splitting decreases by 2.5% in the ~12 h following the injection with the biggest decrease occurring within 2 h. These measurements appear to be very accurate.
   (2) No direct interpretation of the decrease is proposed but it is suggested that the decrease is associated with stress release by the induced events.

   Comments. The observations are generally consistent with the effects of fluid-injection as observed elsewhere [35], except that the recorded shear-wave velocity anisotropy is exceptionally low. Typical values elsewhere are 1.5–4.5% in intact rock, or greater in areas of high heat-flow [5,7]. A major difference is that *Angerer et al. [35] used a controlled source, whereas *Bokelmann and Harjes [36] used injection-induced micro-earthquakes. The probable explanation of both the exceptionally low values of anisotropy and the decrease in time-delays is that the critically-high pore-fluid pressures on the seismically-active faults of the injection-induced events cause 90°-flips in the shear-wave polarisation near the source [44,45]. This means that in highly pressurised rocks, very close to the small seismically-active fault-planes, shear-wave splitting time-delays have negative values. The sum of the larger positive fixed time-delays along the normally pressurised remainder of the path to the borehole recorder, ~4000 m above the seismic events, with small but increasing

negative time-delays means that the initial time-delay decreases with time. Fallacies [F9] and [F12] contribute to the original interpretation.

E.2.3. Oil field production: *Teanby et al. [37] [R1, R2, R3]

*Teanby et al. [37] analyse borehole recordings of two separate clusters of microseismic events induced by production processes in a North Sea oil reservoir. The two clusters show approximately orthogonal polarisations at a 100-m string of geophones in a single well some 250-m above the clusters of earthquakes. These polarisations were interpreted as the effect of three-dimensional variations of polarisations above distributions of parallel vertical fluid-saturated microcracks, as expected theoretically for propagation through thin parallel vertical fluid-saturated microcracks [7].

In addition: "There appears to be a superficial temporal correlation between variations in per cent anisotropy, seismicity and ocean tides." The most important overall conclusion is that it is possible to monitor changes in crack properties induced by changes in pore pressure and/or stress during hydrocarbon production processes.

Comments. Similar to *Angerer et al. [35], *Teanby et al. [37] is another oil field demonstration that shear-wave splitting can monitor pressure- and stress-induced changes to microcrack geometry. To our knowledge, this is the first observation of (possible) changes in shear-wave splitting associated with tides. Another detailed borehole measurement of shear-wave arrival times onshore in Iceland [38] (next section) did not show tidal changes. The reason for this difference is not wholly understood but one factor may be that the ray paths of *Teanby et al. [37] tend towards vertical, whereas the ray paths [38] are strictly horizontal. Another factor may be that the observations in Iceland were at 500-m depth, whereas the KTB well geophones were much deeper at ∼4000 m.

E.2.4. SMSITES experiment: *Crampin et al. [38] [R1, R3, R5, R6]

*Crampin et al. [38] report the SMSITES experiment between boreholes in Northern Iceland where controlled source cross-hole seismics recorded P-, SV-, and SH-wave travel times, SV–SH travel times, horizontally at 500-m depth between boreholes 315-m apart, in directions parallel to and offset ∼100 m from the Húsavík-Flatey Fault (HFF), where it runs onshore in North-Central Iceland. HFF is a transform fault of the Mid-Atlantic Ridge. Also recorded were well-pressures in a water-well on Flatey Island immediately above the HFF, and NS and EW Global Positioning-system (GPS) measurements of horizontal displacements. Repeated sweeps of the Downhole Orbital Vibrator (DOV) source [134,135] every 12–20 s, were stacked every 100 sweeps continuously for 13 days (11–24 August 2001). All seven parameters: four seismic (P-, SH-, SV-, and SV-SH travel times), water-well level, and NS and EW GPS measurements showed well-recorded anomalies coinciding exactly with the onset of a swarm of 106 small ($M_L < 2.8$) earthquakes 70-km distant on a neighbouring transform fault [38]. The total seismic energy was approximately equivalent to one M_L 3.5 earthquake with a source radius of ∼100 m, at most, which is a small earthquake. Thus the sensitivity at SIMITES to low-level seismicity at several hundred times the effective source diameter is far beyond that expected in a brittle-elastic upper crust, and is believed to be direct evidence for the sensitivity expected in critical-systems of fluid-saturated cracks [41–43].

E.2.5. Geothermal Field I: *Crampin and Booth [39] [R1, R4]

*Crampin and Booth [39] observed, small but consistent, 7° changes in shear-wave polarisations at the surface between those from small acoustic events induced by an initial low-pressure water-injection, when equipment was being tested, and those induced by routine hydraulic fracturing operations in a hot-dry-rock geothermal-heat experiment by Cambourne School of Mines at Rosemanowes Quarry in Cornwall, UK. The initial polarisations were parallel to stress directions measured by overcoring techniques at depth, whereas the polarisations of the hydraulic fracturing induced events were parallel to joints and fractures in granite in surface outcrops. This was interpreted as pumping-induced hydraulic dilation of pre-existing joints in the granite.

Comments. The separation between stress directions and pre-existing joints suggests that hydraulic fracturing in low-porosity crystalline rocks may open existing joints and fractures in preference to wholly stress-aligned fractures, when they are separated by only a small angle. It is interesting that observations of

shear-wave splitting away these induced events on seismically-active faults appear to be highly accurate [35], can be calculated with APE, and avoid the ±80% scatter associated with earthquake sources.

E.2.6. Geothermal Field II: *Tang et al. [40] [R1], [F6]

*Tang et al. [40] report large values of time-delays (normalised by path length) above small events in two regions of high heat-flow: close to fluid-injection wells near the Krafla Volcano, Iceland; and near the Cocos Geothermal Field, California. In both cases the values of normalised time-delays are exceptionally high (greater than 25 ms/km) during the fluid-injection. When the injection was stopped, the normalised time-delays dropped to less than ~20 ms/km, which is typical of the values elsewhere in Iceland where it is attributed to the effects of high heat-flow [5,46]. Typical values in areas without high heat-flow are usually less than 8 ms/km, some times less than 4 ms/km [7]. *Tang et al. [40] do not give any physical explanation for the high values, but suggest that they are monitoring the effects of changes in fluid pressures. *Tang et al. also show rose-diagrams of shear-wave polarisations which appear to show a wide range of different polarisations. All time-delays show the typical ±80% always associated with measurements above earthquakes [45].

Comments. The only viable explanation for the larger time-delays during injection is spatial variations. The events during injection with large normalised time-delays are identified as being close to and above the injection points at both Krafla and Cocos [40]. Cracks at very shallow depths under greatly-reduced lithostatic pressure are likely to have higher crack densities than deeper cracks, and the shorter ray paths in the normalisation would exaggerate any minor increase in time-delays.

Note that the rose-diagrams in *Tang et al. [40] are in *equal-degree* polar projections which accentuate any preferential alignment as larger petals are preferentially over-weighted. Plotted in *equal-area rose*-diagrams, as in [5,7], the rose-diagrams of *Tang et al. would show less alignment and a much higher degree of scattering. The topography of the Krafla seismic network is irregular with many abrupt 22° to 14° slopes which would seriously disturb the edge of the shear-wave widow. Everywhere else, oddly aligned or scattered polarisations can typically be explained by topographic irregularities [5,7].

References

Papers where temporal variations in shear-wave splitting time-delays have been identified either by the authors or by re-interpretations in this review, †Papers available at <http://www.geos.ed.ac.uk/homes/scrampin/opinion>

[1] S. Crampin, A review of wave motion in anisotropic and cracked elastic-media, Wave Motion 3 (1981) 343–391.
[2] *†S. Crampin, The fracture-criticality of crustal rocks, Geophys. J. Int. 118 (1994) 428–438.
[3] *S. Crampin, Anisotropists Digest 149 and 150, anisotropists@sep.stanford.edu (1996).
[4] *D. Winterstein, Anisotropists Digest 147, anisotropists@sep.stanford.edu (1996).
[5] *†T. Volti, S. Crampin, A four-year study of shear-wave splitting in Iceland: 2. Temporal changes before earthquakes and volcanic eruptions, in: D.W. Nieuwland (Ed.), New Insights into Structural Interpretation and Modelling, vol. 212, Geol. Soc. Lond., Spec. Publ., London, 2003, pp. 135–149.
[6] *†Y. Gao, S. Crampin, Observations of stress relaxation before earthquakes, Geophys. J. Int. 157 (2004) 578–582.
[7] †S. Crampin, Calculable fluid-rock interactions, J. Geol. Soc. 156 (1999) 501–514.
[8] S. Crampin, R. Evans, B. Üçer, M. Doyle, J.P. Davis, G.V. Yegorkina, A. Miller, Observations of dilatancy-induced polarization anomalies and earthquake prediction, Nature 286 (1980) 874–877.
[9] M. Ando, Y. Ishikawa, H. Wada, S-wave anisotropy in the upper-mantle under a volcanic area in Japan, Nature 286 (1980) 43–46.
[10] †S. Crampin, S. Peacock, A review of shear-wave splitting in the compliant crack-critical anisotropic Earth, Wave Motion 41 (2005) 59–77.
[11] †S. Crampin, The New Geophysics: a new understanding of fluid-rock deformation, in: A. Van Cotthem, R. Charlier, J.-F. Thimus, J.-P. Tshibangu (Eds.), Eurock 2006: Multiphysics Coupling and Long Term Behaviour in Rock Mechanics, Taylor & Francis, London, 2006, pp. 539–544.
[12] S. Crampin, R. Evans, S.B. Üçer, Analysis of records of local earthquakes: the Turkish Dilatancy Projects (TDP1 and TDP2), Geophys. J.R. Astron. Soc. 83 (1985) 1–16 (see also pages: 17–30; 31–46; 47–60; 61–74; and 75–92).
[13] R.M. Alford, Shear data in the presence of azimuthal anisotropy, Dilley, Texas, 56th Ann. Int. Mtg., Soc. Expl. Geophys. Houston (1986) 379–476, Expanded Abstracts.
[14] M.C. Mueller, Prediction of lateral variability in fracture intensity using multicomponent shear-wave surface seismic as a precursor to horizontal drilling in the Austin chalk, Geophys. J. Int. 107 (1991) 409–415.
[15] K. Helbig, L. Thomsen, 75-plus years of anisotropy in exploration and reservoir seismics: a historical review of concepts and methods, Geophysics 70 (2006) 9ND–23ND.

[16] [†]Y. Gao, P. Hao, S. Crampin, SWAS: a shear-wave analysis system for semi-automatic measurement of shear-wave splitting above small earthquakes, Phys. Earth. Planet. Inter. 159 (2006) 71–89.

[17] P. Davis (Ed.), The New Physics, Cambridge University Press, 1989.

[18] P. Davis, The New Physics: a synthesis, in: P. Davis (Ed.), The New Physics, Cambridge University Press, Cambridge, 1989, pp. 1–6.

[19] A. Bruce, D. Wallace, Critical point phenomena: universal physics at large length scale, in: P. Davis (Ed.), The New Physics, Cambridge University Press, Cambridge, 1989, pp. 236–267.

[20] N. Barton, Rock Quality, Seismic Velocity, Attenuation and Anisotropy, Taylor & Francis, London, 2007.

[21] [*]Y. Gao, P. Wang, S. Zheng, M. Wang, Y.-T. Chen, Temporal changes in shear-wave splitting at an isolated swarm of small earthquakes in 1992 near Dongfang, Hainan Island, Southern China, Geophys. J. Int. 135 (1998) 102–112.

[22] [*]D.C. Booth, S. Crampin, J.H. Lovell, J.-M. Chiu, Temporal changes in shear wave splitting during an earthquake swarm in Arkansas, J. Geophys. Res. 95 (1990) 11151–11164.

[23] [*]Y. Liu, S. Crampin, I. Main, Shear-wave anisotropy: spatial and temporal variations in time delays at Parkfield, Central California, Geophys. J. Int. 130 (1997) 771–785.

[24] [*†]Y. Gao, S. Crampin, A further stress-forecast earthquake (with hindsight), where migration of source earthquakes causes anomalies in shear-wave polarizations, Tectonophysics 426 (2006) 253–262.

[25] [*†]S. Crampin, T. Volti, R. Stefánsson, A successfully stress-forecast earthquake, Geophys. J. Int. 138 (1999) F1–F5.

[26] [*]Y. Gao et al., Changes in characteristics of shear-wave splitting of earthquakes in Shidian, Yunnan, China, Acta Seism. Sinica 17 (2004) 635–641.

[27] [*]S. Peacock, S. Crampin, D.C. Booth, J.B. Fletcher, Shear-wave splitting in the Anza seismic gap, Southern California: temporal variations as possible precursors, J. Geophys. Res. 93 (1988) 3339–3356.

[28] [*]S. Crampin, D.C. Booth, R. Evans, S. Peacock, J.B. Fletcher, Changes in shear wave splitting at Anza near the time of the North Palm Springs Earthquake, J. Geophys. Res. 95 (1990) 11197–11212.

[29] [*]S. Crampin, D.C. Booth, R. Evans, S. Peacock, J.B. Fletcher, Comment on "Quantitative measurements of shear wave polarizations at the Anza seismic network, Southern California: implications for shear wave splitting and earthquake prediction" by R.C. Aster, P.M. Shearer, J. Berger, J. Geophys. Res. 96 (1991) 6403–6414.

[30] [*]J. Wu, Y. Gao, S. Crampin, T. Volti, Y.-T. Chen, Smaller source earthquakes and improved measuring techniques allow the largest earthquakes in Iceland to be stress-forecast (with hindsight), Geophys. J. Int. 166 (2006) 1293–1298.

[31] [*†]S. Crampin, Y. Gao, Comment on "Systematic analysis of shear-wave splitting in the aftershock zone of the 1999 Chi–Chi, Taiwan, earthquake: shallow crustal anisotropy and lack of precursory changes, by Liu, Teng, Ben-Zion, Bull. Seismol. Soc. Am. 95 (2005) 354–360.

[32] [*]F. Bianco, L. Scarfi, E. Del Pezzo, D. Patanè, Shear wave splitting time variation by stress-induced magma uprising at Mt. Etna volcano, Geophys. J. Int. 167 (2006) 959–967.

[33] [*]V. Miller, M. Savage, Changes in seismic anisotropy after volcanic eruptions: evidence from Mount Ruapehu, Science 293 (2001) 2231–2235.

[34] [*]T.L. Davis, R.D. Benson, S.L. Roche, D. Talley, 4-D 3-C seismology and dynamic reservoir characterization – a geophysical renaissance, 67th Ann. Mtg. Soc. Explor. Geophys., Dallas 1 (1997) 880–882 (Expanded Abstracts, see also 883–885, 886–889).

[35] [*†]E. Angerer, S. Crampin, X.-Y. Li, T.L. Davis, Processing, modelling, and predicting time-lapse effects of overpressured fluid-injection in a fractured reservoir, Geophys. J. Int. 149 (2002) 267–280.

[36] [*]G.H.R. Bokelmann, H.-P. Harjes, Evidence for temporal variation of seismic velocity within the upper continental crust, J. Geophys. Res. 105 (2000) 23879–23894.

[37] [*]N. Teanby, J.-M. Kendall, R.H. Jones, O. Barkved, Stress-induced temporal variations in seismic anisotropy observed in microseismic data, Geophys. J. Int. 156 (2004) 459–466.

[38] [*†]S. Crampin, S. Chastin, Y. Gao, Shear-wave splitting in a critical crust: III – preliminary report of multi-variable measurements in active tectonics, J. Appl. Geophys. 54 (2003) 265–277 (Spec. Issue).

[39] [*†]S. Crampin, D.C. Booth, Shear-wave splitting showing hydraulic dilation of pre-existing joints in granite, Sci. Drilling 1 (1989) 21–26.

[40] [*]C. Tang, J.A. Rial, J.M. Lees, Shear-wave splitting: a diagnostic tool to monitor fluid pressure in geothermal fields, Geophys. Res. Lett. 32 (2005) L21317, doi:10.1029/2005GL023551.

[41] [†]S.V. Zatsepin, S. Crampin, Modelling the compliance of crustal rock: I – response of shear-wave splitting to differential stress, Geophys. J. Int. 129 (1997) 477–494.

[42] [†]S. Crampin, S.V. Zatsepin, Modelling the compliance of crustal rock: II – response to temporal changes before earthquakes, Geophys. J. Int. 129 (1997) 495–506.

[43] [†]S. Crampin, S. Chastin, A review of shear-wave splitting in the crack-critical crust, Geophys. J. Int. 155 (2003) 221–240.

[44] [†]S. Crampin, T. Volti, S. Chastin, A. Gudmundsson, R. Stefánsson, Indication of high pore-fluid pressures in a seismically-active fault zone, Geophys. J. Int. 151 (2002) F1–F5.

[45] S. Crampin, S. Peacock, Y. Gao, S. Chastin, The scatter of time-delays in shear-wave splitting above small earthquakes, Geophys. J. Int. 156 (2004) 39–44.

[46] [*†]T. Volti, S. Crampin, A four-year study of shear-wave splitting in Iceland: 1. Background and preliminary analysis, in: D.W. Nieuwland (Ed.), New Insights into Structural Interpretation and Modelling, vol. 212, Geol. Soc. Lond., Spec. Publ., 2003, pp. 117–133.

[47] [*]A. Gerst, M. Savage, Seismic anisotropy beneath Ruapehu volcano: a possible eruption forecasting tool, Science 306 (2004) 1543–1547.

[48] T.M. Brocher, N.I. Christensen, Seismic anisotropy due to preferred mineral orientation observed in shallow crustal rocks in southern Alaska, Geology 18 (1989) 737–740.

[49] A.F. do Nascimento, R.G. Pearce, M.K. Takeya, Local shear wave observations in João Câmara, northeast Brazil, J. Geophys. Res. 107 (2002) 2232, doi:10.1029/2001JB000560.

[50] *Y. Liu, T.-L. Teng, Y. Ben-Zion, Systematic analysis of shear-wave splitting in the aftershock zone of the 1999 Chi–Chi, Taiwan, Earthquake: shallow crustal anisotropy and lack of precursory changes, Bull. Seismol. Soc. Am. 94 (2004) 2330–2347.

[51] S. Crampin, Comment and reply on "Seismic anisotropy due to preferred mineral orientation observed in shallow crustal rocks in southern Alaska" by T.M. Brocher, N.I. Christensen, Geology 19 (1991) 859–860.

[52] †S. Crampin, Comments on "Local shear wave observations in João Câmara, northeast Brazil" by A.F. do Nascimento, R.G. Pearce, M.K. Takeya, J. Geophys. Res. 109 (2004) B02313, doi:10.1029/2003JB002681.

[53] A.F. do Nascimento, R.G. Pearce, M.K. Takeya, Reply to comments by Crampin, S. on "Local shear wave observations in João Câmara, northeast Brazil", J. Geophys. Res. 109 (2004) B023104, doi:10.1029/2003JB002754.

[54] *K.R. Gledhill, Evidence for shallow and pervasive seismic anisotropy in the Wellington Region, New Zealand, J. Geophys. Res. 96 (1991) 21503–21516.

[55] W.B. Menke, B. Brandsdottir, S. Jakobsdottir, R. Stefansson, Seismic anisotropy in the crust at the mid-Atlantic plate boundary in south-west Iceland, Geophys. J. Int. 119 (1994) 783–790.

[56] *Y. Liu, Y. Ben-Zion, T.-L. Teng, Reply to "Comments on 'Systematic analysis of shear-wave splitting in the aftershock zone of the 1999 Chi–Chi, Taiwan, Earthquake: shallow crustal anisotropy and lack of precursory changes,' by Y. Liu, T.-L. Teng, Y. Ben-Zion," by S. Crampin, Y. Gao, Bull. Seismol. Soc. Am. 95 (2005) 361–366.

[57] R. Aster, P. Shearer, J. Berger, Quantitative measurements of shear-wave polarizations at the Anza seismic network, southern California: implications for shear-wave splitting and earthquake prediction, J. Geophys. Res. 95 (1990) 12449–12473.

[58] R.C. Aster, P.M. Shearer, J. Berger, Reply, J. Geophys. Res. 96 (1991) 6415–6419.

[59] †S. Crampin, Y. Gao, A review of techniques for measuring shear-wave splitting above small earthquakes, Phys. Earth. Planet. Inter. 159 (2006) 1–14.

[60] T. Seher, I.G. Main, A statistical evaluation of a 'stress-forecast' earthquake, Geophys. J. Int. 157 (2004) 187–193.

[61] *†S. Crampin, T. Volti, R. Stefánsson, Response to "A statistical evaluation of a 'stress-forecast' earthquake" by T. Seher, I.G. Main, Geophys. J. Int. 157 (2004) 194–199.

[62] F.K. Levin, Seismic velocities in transversely isotropic media I, Geophysics 44 (1979) 918–936.

[63] F. Levin, Seismic velocities in transversely isotropic media II, Geophysics 45 (1980) 3–17.

[64] I. Tsvankin, Seismic Signatures and Analysis of Reflection Data in Anisotropic Media, Pergamon, Amsterdam, 2001.

[65] E.A. Kaarsberg, Introductory studies of natural and artificial argillaceous aggregates by sound propagation and X-ray diffraction methods, J. Geol. 67 (1959) 447–472.

[66] E.A. Kaarsberg, Elasticity studies of isotropic and anisotropic rock, Trans. Soc. Min. Eng. 241 (1968) 470–475.

[67] A.M. Dziewonski, D.L. Anderson, Preliminary reference earth model (PREM), Phys. Earth Planet. Inter. 25 (1981) 297–356.

[68] S. Crampin, S.C. Kirkwood, Velocity variations in systems of anisotropic symmetry, J. Geophys. 49 (1981) 35–42.

[69] S. Crampin, Arguments for EDA, Can. J. Expl. Geophys. 29 (1993) 18–30.

[70] S. Crampin, R. Evans, B.K. Atkinson, Earthquake prediction: a new physical basis, Geophys. J.R. Astron. Soc. 76 (1984) 147–156.

[71] W.A. Deer, R.A. Howie, J. Zussman, An Introduction to the Rock-Forming Minerals, Longman, London, 1996.

[72] S. Crampin, D. Bamford, Inversion of P-wave velocity anisotropy, Geophys. J.R. Astron. Soc. 49 (1977) 123–132.

[73] N.I. Christensen, Compressional wave velocities in metamorphic rocks at pressures to 10 kilobars, J. Geophys. Res. 70 (1965) 6147–6164.

[74] N.I. Christensen, Shear wave velocities in metamorphic rocks at pressures to 10 kilobars, J. Geophys. Res. 71 (1966) 3549–3556.

[75] V. Babuška, P-wave velocity anisotropy in crystalline rocks, Geophys. J.R. Astron. Soc. 76 (113) (1984) 1–11.

[76] K.S. Alexandrov, T.V. Ryzhova, Elastic properties of rock-forming minerals: 2. Layered silicates, Bull. Acad. Sci. USSR, Geophys. Ser., English Transl. 12 (1961) 871–875.

[77] M.K. Hubbert, W.W. Rubey, Role of fluid pressure in mechanics of overthrust faulting. 1. Mechanics of fluid filles porous solids and its application to overthrust faulting, Geol. Soc. Am. Bull. 70 (1959) 115–166.

[78] S. Crampin, D.W. King, Evidence for anisotropy in the upper-mantle beneath Eurasia from generalized higher mode surface waves, Geophys. J.R. Astron. Soc. 49 (1977) 59–85.

[79] O. Nuttli, The effects of the Earth's surface on the S-wave particle motion, Bull. Seismol. Soc. Am. 51 (1961) 237–246.

[80] R. Evans, Effects of the free surface on shear wavetrains, Geophys. J.R. Astron. Soc. 76 (1984) 165–172.

[81] D.C. Booth, S. Crampin, Shear-wave polarizations on a curved wavefront at an isotropic free-surface, Geophys. J.R. Astron. Soc. 83 (1985) 31–45.

[82] E. Liu, S. Crampin, Effects of the internal shear wave window: comparison with anisotropy induced splitting, J. Geophys. Res. 95 (1990) 11275–11281.

[83] S. Crampin, A review of the effects of crack geometry on wave propagation through aligned cracks, Can. J. Expl. Geophys. 29 (1993) 3–17.

[84] Z. Peng, Y. Ben-Zion, Systematic analysis of crustal anisotropy along the Karadere-Düzce branch of the North Anatolian fault, Geophys. J. Int. 159 (2004) 253–274.

[85] R. Stefánsson et al., Earthquake prediction research in the South Iceland Seismic Zone and the SIL Project, Bull. Seismol. Soc. Am. 83 (1993) 696–716.

[86] S. Crampin et al., SMSITES: developing stress-monitoring sites and infrastructure for forecasting earthquakes, Final Report to European Commission, EC Contract No. EVR1-CT1999-40002, 2004, p. 73.

[87] S. Crampin, Effective anisotropic elastic-constants for wave propagation through cracked solids, Geophys. J.R. Astron. Soc. 76 (1984) 135–145.

[88] S. Crampin, Seismic wave propagation through a cracked solid: polarization as a possible dilatancy diagnostic, Geophys. J.R. Astron. Soc. 53 (1978) 467–496.

[89] J.A. Hudson, Overall properties of a cracked solid, Math. Proc. Camb. Phil. Soc. 88 (1980) 371–384.

[90] J.A. Hudson, Wave speeds and attenuation of elastic waves in material containing cracks, Geophys. J.R. Astron. Soc. 64 (1981) 133–150.

[91] [*][†]S. Crampin, The New Geophysics: shear-wave splitting provides a window into the crack-critical rock mass, Leading Edge 22 (2003) 536–549.

[92] S. Crampin, Shear-wave splitting in a critical self-organized crust: the New Geophysics, 70th Ann. Int. Mtg., Soc. Expl. Geophys. Calgary 2 (2000) 1544–1547, Expanded Abstracts.

[93] S. Crampin, M. Yedlin, Shear-wave singularities of wave propagation in anisotropic media, J. Geophys. 49 (1981) 43–46.

[94] S. Crampin, Effects of point singularities on shear-wave propagation in sedimentary basins, Geophys. J. Int. 107 (1991) 531–543.

[95] S. Crampin, S.V. Zatsepin, C. Slater, L.Y. Brodov, Abnormal shear-wave polarizations as indicators of pressures and over pressures, 58th Conf., EAGE, Amsterdam, Extended Abstracts, X038 (1996).

[96] I. Bush, S. Crampin, Paris Basin VSPs: case history establishing combinations of matrix- and crack-anisotropy from modelling shear wavefields near point singularities, Geophys. J. Int. 107 (1991) 433–447.

[97] S. Crampin, D.C. Booth, M.A. Krasnova, E.M. Chesnokov, A.B. Maximov, N.T. Tarasov, Shear-wave polarizations in the Peter the First Range indicating crack-induced anisotropy in a thrust-fault regime, Geophys. J.R. Astron. Soc. 84 (1986) 401–412.

[98] G.M. Holmes, S. Crampin, R.P. Young, Seismic anisotropy in granite at the Underground Research Laboratory, Manitoba, Geophys. Prosp. 48 (2000) 415–435.

[99] [*]Y.-G. Li, T.-L. Teng, T.L. Henyey, Shear-wave splitting observations in the Northern Los Angeles Basin, Southern California, Bull. Seismol. Soc. Am. 84 (1994) 307–323.

[100] [*]R.M. Nadeau, W. Foxall, T.V. McEvilly, Clustering and periodic recurrence of microearthquakes on the San Andreas Fault at Parkfield, California, Science 267 (1995) 503–507.

[101] [*]E. Karageorgi, T.V. McEvilly, R. Clymer, P. Source, Seismological studies at Parkfield. IV: variations in controlled-source waveform parameters and their correlation with seismicity, 1987 to 1995, Bull. Seismol. Soc. Am. 87 (1997) 39–49.

[102] [*]K.R. Gledhill, Shear waves recorded on close-spaced seismographs: I. Shear-wave splitting results, Can. J. Expl. Geophys. 29 (1993) 285–298.

[103] N.J. Balfour, M.K. Savage, J. Townend, Stress and crustal anisotropy in Marlborough, New Zealand: evidence for low fault strength and structure-controlled anisotropy, Geophys. J. Int. 163 (2005) 1073–1086.

[104] [*]E. Del Pezzo, F. Bianco, S. Petrosino, G. Saccorotti, Changes in the coda decay rate and shear-wave splitting parameters associated with seismic swarms at Mt. Vesuvius, Italy, Bull. Seismol. Soc. Am. 94 (2004) 439–452.

[105] [*]A. Saiga, Y. Hiramatsu, T. Ooida, K. Yamaoka, Spatial variation in the crustal anisotropy and its temporal variation associated with a moderate-sized earthquake in the Tokai region, Geophys. J. Int. 154 (2003) 695–705.

[106] G. Graham, S. Crampin, Shear-wave splitting from regional earthquakes in Turkey, Can. J. Expl. Geophys. 29 (1993) 279–371.

[107] G.V. Yegorkina, V.A. Rakitov, I.V. Garetovskaya, L.M. Yegorova, Anisotropy of velocities of seismic waves and the stress state of the Earth's crust in the territory of Armenia, Izvestiya, Earth Phys. (English Ed.) 13 (1977) 554–562.

[108] W.M. Kohler, J.H. Healy, S.S. Wegner, Upper crustal structure of the Mount Hood, Oregon, Region as revealed by time-term analysis, J. Geophys. Res. 87 (1982) 339–355.

[109] S. Crampin, R. McGonigle, M. Ando, Extensive-dilatancy anisotropy beneath Mount Hood, Oregon, and the effect of aspect ratio on seismic velocities through aligned cracks, J. Geophys. Res. 91 (1986) 12703–12710.

[110] C.W. Burnham, J.R. Holloway, N.F. Davis, Thermodynamic properties of water to 1,000°C and 10,000 bars, Spec. Paper, Geol. Soc. Am. 132 (1969) 36.

[111] S. Crampin, Aligned cracks not LPO as the cause of mantle anisotropy, EGS-AGU-EUG Joint Assembly, 06–11 April, 2003, Nice, EAEG03-A-00205, SM4-1FR1P-0073, 2003.

[112] J.B. Fletcher, T. Fumal, H.-P. Liu, L.C. Carrol, Near-surface velocities and attenuation at two boreholes near Anza, California, from logging data, Bull. Seismol. Soc. Am. 80 (1990) 807–831.

[113] T.M. Daley, T.V. McEvilly, Shear wave anisotropy in the Parkfield Varian Well VSP, Bull. Seismol. Soc. Am. 80 (1990) 857–869.

[114] R.C. Aster, P.M. Shearer, High-frequency borehole seismograms recovered in the San Jacinto Fault Zone, Southern California. Part 1. Polarisations, Bull. Seismol. Soc. Am. 81 (1991) 1057–1080.

[115] P. Leary, R.E. Abercrombie, Frequency dependent crustal scattering and absorption at 5–160 Hz from coda decay observed at 2.5 km depth, Geophys. Res. Lett. 21 (1994) 971–974.

[116] R.C. Aster, P.M. Shearer, Initial shear wave particle motions and stress constraints at the Anza Seismic Network, Geophys. J. Int. 108 (1992) 740–748.

[117] Z. Zhang, S.Y. Schwartz, Seismic anisotropy in the shallow crust of the Loma Prieta segment of the San Andreas fault system, J. Geophys. Res. 100 (1994) 9651–9661.

[118] S. Crampin, The scattering of shear waves in the crust, Pure Appl. Geophys. 132 (1990) 67–91.

[119] J.C. Zinke, M.D. Zoback, Structure-related and stress-induced shear-wave velocity anisotropy: observations from microearthquakes near the Calaveras Fault in central California, Bull. Seismol. Soc. Am. 90 (2000) 1305–1312.

[120] X.R. Shih, R.P. Meyer, Observation of shear wave splitting from natural events: South Moat of Long Valley Caldera, California, June 29 to August 12, 1982, J. Geophys. Res. 95 (1990) 11179–11195.

[121] E.S. Cochran, J.E. Vidale, Y.-G. Li, Near-fault anisotropy following the Hector Mine earthquake, J. Geophys. Res. 108 (B9) (2003) 2436, doi:10.1029/2002JB002352.

[122] C.G. Munson, C.H. Thurber, Y. Li, P.G. Okuba, Crustal shear wave anisotropy in southern Hawaii: spatial and temporal analysis, J. Geophys. Res. 99 (1995) 20367–20377.

[123] S. Kaneshima, Origin of crustal anisotropy: shear wave splitting studies in Japan, J. Geophys. Res. 95 (1990) 11121–11123.

[124] T. Volti, Y. Kaneda, S. Zatsepin, S. Crampin, Shear-wave splitting in Nankai Trough (Japan) using ocean bottom seismometers and HINET data, in: Frontier Research on Earth Evolution, IFREE Rep. 2001–2002, 1 (2003) 155–167.

[125] *Y. Hiramatsu, H. Honma, A. Saiga, M. Furumoto, T. Ooida, Seismological evidence on characteristic time of crack healing in the shallow crust, Geophys. Res. Lett. 32 (2005) L09304, doi:10.1029/2005GL022656.

[126] M.A. Krasnova, E.M. Chesnokov, Changes in shear-wave polarization in the crust of Kamchatka based on records of local earthquakes, Volc. Seismol. 20 (1999) 539–550.

[127] M.N. Luneva, J.M. Lee, Shear wave splitting beneath South Kamchatka during the 3-year period associated with the 1997 Kronotsky earthquake, Tectonophysics 274 (2003) 135–161.

[128] *K.R. Gledhill, Shear waves recorded on close-spaced seismographs: II. The complex anisotropic structure of the Wellington Peninsula, New Zealand, Can. J. Expl. Geophys. 29 (1993) 299–314.

[129] E. Audoine, M.K. Savage, K. Gledhill, Seismic anisotropy form local earthquakes in the transition region from a subduction to a strike-slip plate boundary, New Zealand, J. Geophys. Res. 105 (2000) 8013–8033.

[130] E. Audoine, M.K. Savage, K. Gledhill, Anisotropic structure under a back arc spreading region, the Taupo Volcanic Zone, New Zealand, J. Geophys. Res. 109 (2004) B11305, doi:10.1029/2003JB:002932.

[131] D.B. Taylor, Double contour integration for transmission from point sources through anisotropic layers as used in ANISEIS software, Geophys. J.R. Astron. Soc. 91 (1987) 373–381.

[132] D.B. Taylor, ANISEIS Manual, Version 5.6, MACROC Ltd. Available from: <http://xweb.geos.ed.ac.uk/~ernm01/anis/Manual.html> (2005).

[133] M.D. Zoback, H.-P. Harjes, Injection-induced earthquakes and crustal stress at 9 km depth at the KTB deep drilling site, Germany, J. Geophys. Res. 102 (1997) 18477–18491.

[134] P.C. Leary, L.A. Walter, S. Crampin, Physical model for downhole orbital vibrator (DOV) – (1) acoustic radiation, 73rd Ann. Int. Soc. Explor. Geophys., Mtg, Dallas, 2003, Expanded Abstracts 2 (2003) 1532–1535.

[135] L.A. Walter, P.C. Leary, S. Crampin, Physical model for downhole orbital vibrator (DOV) – (2) seismic radiation, 73rd Ann. Int. Mtg, Soc. Explor. Geophys., Dallas, 2003, Expanded Abstracts 2, 1536–1539 (2003).